The Baeyer-Villiger oxidation versus aromatic ring hydroxylation: competing organic peracid oxidation mechanisms explored by multivariate modelling of designed multi-response experiments

Cristian Gambarotti[a] and Hans-René Bjørsvik[b]*

INTRODUCTION

Phenol derivatives are valuable industrial chemicals[1] used for the synthesis of advanced pharmaceutical intermediates and active pharmaceutical ingredients,[2] for the production of agrochemicals,[3] flavouring and fragrances,[4] monomers for polymers,[5] various antioxidants[6] and numerous of other fine chemical applications and commodity chemicals as well.

Industrial synthesis of phenol is based on the Hock process, which involves autoxidation of cumene.[7] Phenol derivatives can be prepared by means of the Baeyer–Villiger oxidation[8] with a subsequent ester hydrolysis. Access to various phenol derivatives have also been revealed by direct hydroxylation, by peracid oxidation of the aromatic ring[9] and palladium catalysed C–H oxygenation.[10]

Previously, one of our research assignments pertained direct hydroxylation of the benzene ring with the objective to produce the corresponding phenol and their derivatives. The research activity included (1) preparation of methoxy-substituted phenols by oxidation of the corresponding benzenes in one synthetic step, path (iv) of Scheme 1, and (2) synthesis of 2-methoxy-3-methyl-[1,4]benzo-quinone **6** by means of a two-step telescoped process, where the phenol was generated in the first step (not isolated), whereupon the phenolic hydroxyl group was further oxidized by a second oxidant to induce the formation of the resultant quinone derivate.[11] This latter process was afterward adapted for the synthesis of the 2,3-dimethoxy-5-methylcyclohexa-2,5-diene-1,4-dione (also known as CoQ_0)[12] that is an essential building block in the synthesis of ubiquinones (also known as coenzyme Q_n, $n = 1,\ldots, 12$, and mitoquinones), and the synthetic analogue idebenone.[13]

Direct hydroxylation of the benzene ring, step (iv) of Scheme 1, can be of pronounced importance from an industrial point of view when focusing process efficacy, process economy and environmental issues, because an operating alternative encompassing the steps (i–iii) of Scheme 1 that involves a Friedel–Crafts acylation,[14] a Baeyer–Villiger oxidation[8] and an ester hydrolysis.[15] The Baeyer–Villiger oxidation with a successive Fries rearrangement[16] is a pathway frequently utilized for the purpose to introducing a hydroxyl group in the *ortho*-position to an acetyl group. The resulting *ortho*-acetylphenols can serve as versatile building blocks and have been used in the synthesis of carbazomycin G and H[17] and carbazoquinocin C,[18] for the synthesis of natural products and biological activity compounds[19] and in the synthesis of precursors of

* *Correspondence to: Hans-René Bjørsvik, Department of Chemistry, University of Bergen, Allégaten 41, N-5007 Bergen, Norway.*
E-mail: Hans.Bjorsvik@kj.uib.no

a *C. Gambarotti*
Department of Chemistry, Materials and Chemical Engineering, Politecnico di Milano, Piazza Leonardo da Vinci 32, I-20133, Milan, Italy

b *H.-R. Bjørsvik*
Department of Chemistry, University of Bergen, Allégaten 41, N-5007, Bergen, Norway

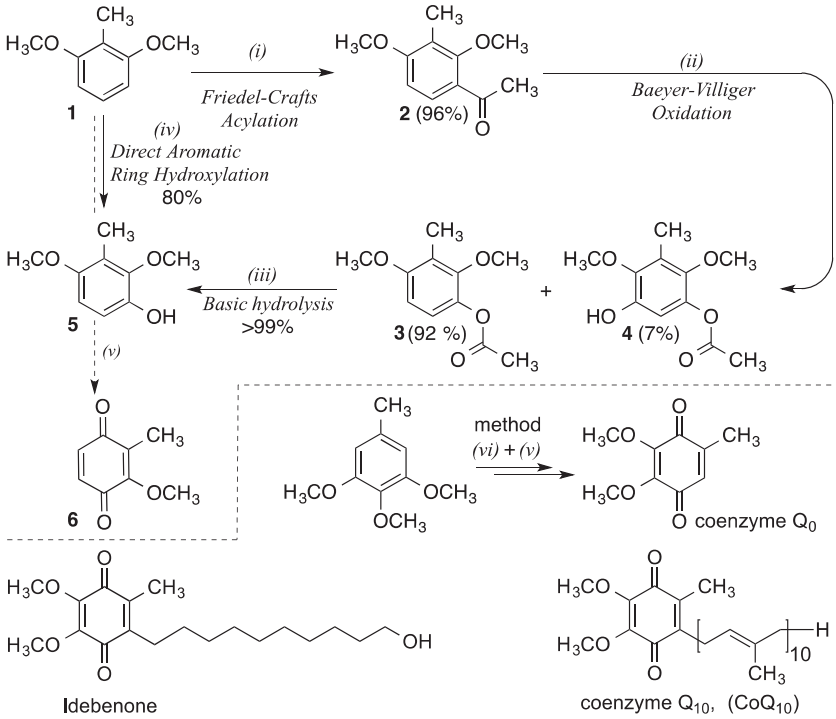

Scheme 1. Two synthetic pathways (i)–(iii) or (iv) that are both leading to 2,4-dimethoxy-3-methylphenol 5 starting from 1,3-dimethoxy-2-methylbenzene 1. Another pathways (iv) and (v) that are also starting from 1,3-dimethoxy-2-methylbenzene 1 that proceed via 2,4-dimethoxy-3-methylphenol **5** as an intermediate to obtain 2-methoxy-3-methylcyclohexa-2,5-diene-1,4-dione **6** as target molecule

anti-tubulin agents.[20] However, the same phenolic precursor can be easily prepared in one step from the appropriate substituted toluene by direct hydroxylation of the aromatic ring.

EXPERIMENTAL

Computing and software

An in-house developed function library (by H. R. B.) for MATLAB (MathWorks, Natick, MA, USA) was used for the multivariate regression and for the productions of the *iso*-contour projections of the response surfaces and other line graphics. This library was used under the MATLAB program version 7.11.0.584 (R2010b), 64-bit (maci64), Date: 16 August 2010 [19] that was run with OS X, Version 10.8.3 (12D78) as the operating system. The in-house developed function library has earlier been benchmarked versus various commercial softwares such as SAS (Institute Inc., Cary, NC, USA). Regression and model assessments were also conducted by means of the SAS software version 9.4 for Windows.

Materials and equipment

2,6-Dimethoxyacetophenone (assay 98%), *meta*-chloroperbenzoic acid (*m*CPBA, technical grade ≈70%), *para*-toluenesulfonic acid monohydrate (purum ≥98%), 1,4-dinitrobenzene (assay 98%), acetonitrile (CHROMASOLV® [Sigma-Aldrich, St. Louis, MO, USA] gradient grade, for high-performance liquid chromatography, ≥99.9%) and propionitrile (purum, ≥99%) were purchased from commercial sources and used without further purification.

Gas chromatography–mass spectrometry (GC-MS) spectra were recorded with an Agilent 6890 (Agilent Technologies, Sta. Clara, CA, USA) gas chromatograph (GC) system equipped with a 30 m × 0.250 mm HP-5MS GC column and an Agilent 5973 mass selective detector (MSD). All the reaction products were known and were thus identified by comparison with literature data. Furthermore, the desired product **9** (new compound) was anyhow isolated and characterized by GC-MS, ^{1}H nuclear magnetic resonance (NMR) and ^{13}C NMR, for which the recorded spectra are included in the supporting information file. The quantification was conducted by means of an internal standard method. The internal standard (100 mg of 1,4-dinitrobenzene) was added to the reaction mixture from the start of the reaction.

A Bruker AV 400 (Billerica, MA, USA) NMR instrument equipped with a 5 mm multinuclear probe with a reverse detection was used to record ^{1}H-NMR spectra (at 400 MHz) and ^{13}C NMR spectra (at 100 MHz).

General experimental procedure that was used for the experimental design

2,6-Dimethoxyacetophenone (1 mmol, 180 mg) was transferred to a round-bottom flask (25 mL) and dissolved in acetonitrile (5 mL). Then *para*-toluenesulfonic acid monohydrate (*p*TSA) (quantity as stated in the experimental design table), *meta*-chloroperbenzoic acid (*m*CPBA, quantity as reported in the experimental design table) and the internal standard 1,4-dinitrobenzene (0.73 mmol) were added to the round-bottom flask. The resulting reaction mixture was heated under continuous vigorous stirring at the temperature as given in the experimental design table. During the first hour of the reaction, samples (0.100 mL) were withdrawn from the reaction mixture every 15 min, filtered through a pad silica gel (1 cm height in a Pasteur pipette) using acetone (3 mL) as solvent and analysed on a GC-MS.

Optimized experimental procedure

2,6-Dimethoxy-acetophenone **7** (1 mmol, 180 mg) was transferred to a round-bottom flask (25 mL) and dissolved with acetonitrile (5 mL). Then Amberlite IR120 (Sigma-Aldrich; acid form, 200 mg), *m*CPBA (1.75 mmol) and the internal standard 1,4-dinitrobenzene (0.73 mmol) were added. The resulting reaction mixture was heated under continuous vigorous stirring at reflux temperature (80 °C). A sample (0.100 mL) was withdrawn at reaction times of 30 and 45 min, filtered over silica gel (1 cm height in a Pasteur pipette) using acetone (3 mL) as solvent and analysed on a GC-MS. All the identified compounds were compared with authentic samples. The reaction produced 1-(3-hydroxy-2,6-dimethoxyphenyl)ethan-1-one **9** in a yield of 73.5% and 2,6-dimethoxyphenyl acetate **8** in a yield of ≈3.5%. Work-up: In order to isolate the phenolic product **9**, the post reaction mixture was diluted by adding water (20 mL), adjusting the pH ≈ 12 by drop-wise addition of 10% NaOH, followed by extracting the side-products (**8**) with dichloromethane (3 × 10 mL). The basic aqueous layer was acidified by adding few drops of conc. HCl (pH < 2), followed by extraction using dichloromethane (3 × 10 mL). The solvent was removed under reduced pressure to obtain the compound **9** in an isolated yield of 65–70% as a yellowish sticky solid.

^{1}H NMR of **9** (400 MHz, $CDCl_3$): δ 2.52 (s, 3 H, CH_3), 3.77 (s, 3 H, CH_3), 3.81 (s, 3 H, CH_3), 5.32 (s, 1 H, OH), 6.59 (d, J = 8.8 Hz, 1 H, CH), 6.92 (d, J = 8.8 Hz, 1 H, CH) ppm.

^{13}C NMR of **9** (100 MHz, $CDCl_3$): δ 32.3, 56.3, 62.9, 107.7, 116.3, 125.5, 143.0, 143.8, 150.0 and 201.8 ppm.

RESULTS AND DISCUSSION

Oxidation of acetophenones – two pathways

When an acetophenone is treated with a peracid (e.g. *m*CPBA), two distinct oxidation mechanisms can take place: (1) the direct hydroxylation of the benzene ring as previously described in an account from our laboratory,[9] a mechanism that we believe involves a direct HO^+ transfer from peracid [R–C(=O)OOH] to the benzene ring of the acetophenone (see pathway ① of Scheme 2) and (2) the well-known Baeyer–Villiger oxidation[8] that involves an oxygen insertion between the acetyl group and the benzene ring of the acetophenone, a reaction sequence that involves the Criegee intermediate[21] (see pathway ② of Scheme 2).

At the outset of our previous studies,[9,11] we followed the procedure reported in the literature (Scheme 1, (i)–(iii)).[22] Together with our target molecule **5**, we observed in addition a side product **4** (<10%). This surprising result, we could only explained by the operation of both of the two distinct mechanisms outlined in Scheme 2. This result spurred us to investigate the possibility to perform a one step direct hydroxylation with 2,6-dimethoxytoluene **1** as substrate to achieve target molecule **5**.

In the present study, we wanted to explore in depth this oxidative system involving peracid with acetophenones as substrate to discern whether it was achievable to control the direction of the oxidation process to either follow pathway ①

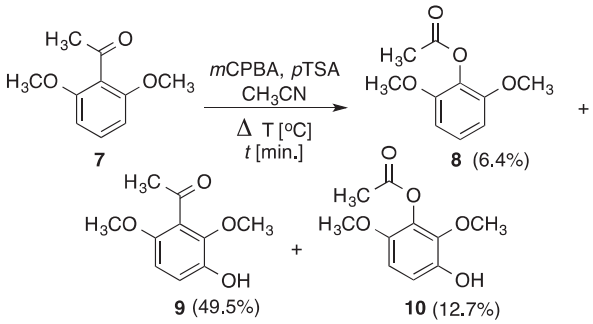

Scheme 3. Direct hydroxylation of the benzene ring versus the Baeyer–Villiger oxidation. Procedure: 2,6-dimethoxyacetophenone (1.0 mmol) was dissolved in CH_3CN (5.0 mL) followed by adding *p*TSA (0.20 mmol) and *m*CPBA (1.0 mmol). The reaction mixture was then leaved under stirring for 1 h at 80 °C (reflux)

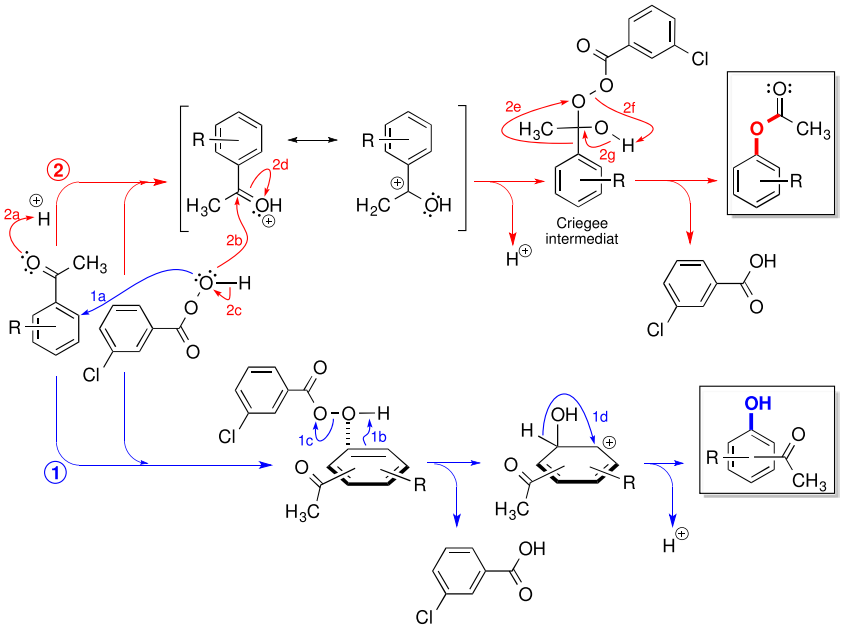

Scheme 2. Proposed mechanisms for the ① direct hydroxylation of the benzene ring using peracid (*m*CPBA) and ② the well-established reaction mechanism for the Baeyer–Villiger oxygen insertion between the actyl group and the benzene ring

Table 1. Statistical experimental design and four different measuring points during the course of the oxidation process

#	Experimental variables[a]			Responses measured by GC by means of internal standard[b]															
				$t = 15$ min				$t = 30$ min				$t = 45$ min				$t = 60$ min			
	x_1	x_2	x_3	y_8	y_9	y_{10}	y	y_8	y_9	y_{10}	y	y_8	y_9	y_{10}	y	y_8	y_9	y_{10}	y
1	−1	−1	−1	0.7	2.3	0.0	0.0	1.2	4.8	0.0	0.0	1.2	8.8	0.0	0.0	1.2	11.8	0.0	0.0
2	+1	−1	−1	1.9	25.6	2.6	0.0	1.6	39	6.7	3.0	2.1	42.6	8.5	5.0	2.2	44.3	10.1	8.0
3	−1	+1	−1	0.5	2.5	0.0	0.0	1.2	5.8	0.0	0.0	1.7	12.3	0.0	0.0	0.8	18.9	1.3	0.0
4	+1	+1	−1	2.5	52.1	7.4	15.0	2.6	52.5	10.5	20.0	1.9	48.7	13.4	28.0	1.9	47.3	13.9	30.0
5	−1	−1	+1	1.5	4.5	0.0	0.0	2.4	7.6	0.0	0.0	3.6	10.2	1.2	0.0	2.9	13.3	1.8	0.0
6	+1	−1	+1	3.5	33.9	6.6	0.0	4.2	42.1	13.8	3.0	4.6	45.4	15.8	6.0	4.6	45.7	15.0	8.0
7	−1	+1	+1	1.1	2.9	0.0	0.0	3.0	9.0	0.0	0.0	2.7	11.2	2.1	0.0	3.3	24.8	5.0	0.0
8	+1	+1	+1	8.7	28.3	6.5	33.0	10.7	25.2	12.6	43.0	9.6	22.8	13.2	50.0	9.3	24.4	15.1	53.0
8[c]	+1	+1	+1	–	–	–	–	11.7	21.0	11.0	43.0	–	–	–	–	–	–	–	–
9	0	0	0	2.3	3.7	0.0	0.0	2.1	11.9	0.0	0.0	5.1	21.3	3.0	0.0	3.4	25.5	5.1	0.0
9[d]	0	0	0	2.6	11.9	1.0	0.0	3.6	26.1	3.3	0.0	4.2	30.4	7.1	3.0	3.7	32.2	10.1	4.0
9[d]	0	0	0	2.3	15.1	1.0	0.0	3.6	28.4	4.0	0.0	3.5	32.7	7.4	3.0	3.4	34.2	11.2	6.0
10[e]	+1	−1.5	+1.5	–	–	–	–	8.7	39.0	8.8	0.0	6.4	49.5	12.7	3.0	6.5	40.4	10.6	15.0

[a]Experimental variables: x_k (Definition) [levels −1, 0 and +1]: x_1 (reaction temperature/°C) [50, 65 and 80]; x_2 : (quantity of *meta*-chloro perbenzoic acid/mmol) [2.0, 2.5 and 3.0]; x_3 : (quantity of *para*-toluene sulphonic acid/mmol) [0.1, 0.2 and 0.3]; t : (reaction time/min) [15, 30, 45 and 60]. Procedure: 2,6-dimethoxy acetophenone (1 mmol) is dissolved in acetonitrile (5 mL) that is added with *m*CPBA and *p*TSA. The reaction mixture is heated at temperature T for a reaction time t.
[b]Responses: yield of $y_{\mathbf{8}}$ = 2,6-dimethoxyphenyl acetate **8**, yield of $y_{\mathbf{9}}$ = 1-(3-hydroxy-2,6-dimethoxyphenyl)ethanone **9** and yield of $y_{\mathbf{10}}$ = 3-hydroxy-2,6-dimethoxyphenyl acetate **10**. Y = %-substance decomposition in total. The response values (yield-%) were measured by means of gas chromatograph (GC) with 1,4-dinitrobenzene as internal standard.
[c]Repeated (parallel) experiment of experiment #8.
[d]Repeated (parallel) experiment of experiment #9.
[e]Experiment that was conducted based on predicted conditions from the *iso*-contour projection of the response surface map in Fig. 2.

or ② (Scheme 2) solely by tuning the experimental variables (experimental condition controlled) or if the favoured mechanistic pathway barely was controlled by the electronic effects (and eventually steric, bulkiness effects) of the substituents on the acetophenone substrate. Introductory screening experiments were performed with 2,6-dimethoxyacetophenone **7** as a model substrate, Scheme 3.

Introductory experiments

At the outset of this investigation, both *in situ* generated peracid using acetic acid with hydrogen peroxide and *m*CPBA were explored. The outcome of these initial trials revealed a lower selectivity and some product degradation when the acetic acid and hydrogen peroxide were used as the oxidative system, which probably is due to the high concentration of the acetic acid (used as solvent) with a large excess of hydrogen peroxide necessary to promote the formation of the peracetic acid. Moreover, the large surplus of hydrogen peroxide may cause subsequent oxidations (over oxidation) of the formed phenolic or ester products.

Three different products were formed during the oxidation of **7**: 2,6-dimethoxy-phenyl acetate **8**, 1-(4-hydroxy-2,6-dimethoxy-phenyl) ethanone **9** and 3-hydroxy-2,6-dimethoxyphenyl acetate **10** (Scheme 3). At the first glance, this primary result was somewhat disappointing as a rather low selectivity was demonstrated. However, from the past experience, we know that fine-tuning of the experimental variables enables one to improve the selectivity of any synthetic reaction. Propelled by this fact, we decided to undertake a methodical investigation of the oxidative conditions involving *m*CPBA by means of a statistical experimental design[23] and multivariate regression using the multiple linear regression[24] method as implemented in the SAS software[25] and by means of the MATLAB software.[26]

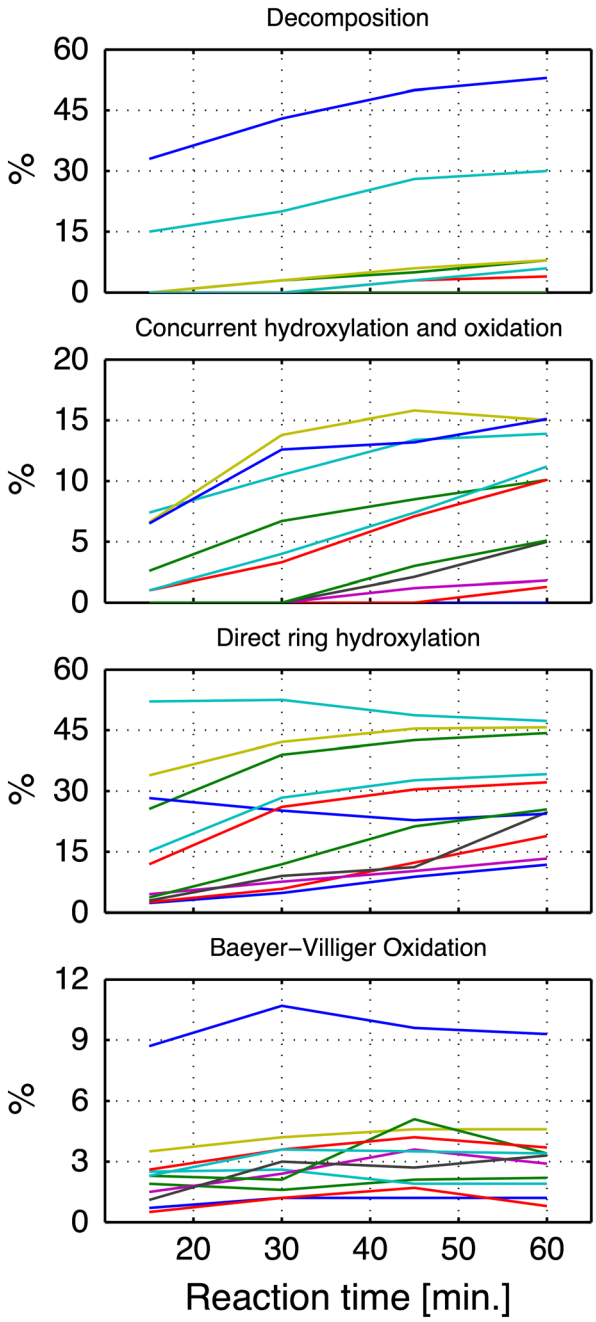

Figure 1. Progress of each single experiment in four responses (y_8, y_9, y_{10} and y) of the experimental design of Table 1. Samples were withdrawn from the reaction mixtures at 15, 30, 45 and 60 min and represented as a line graph for each experiment

Statistical experimental design

Four different measured responses were explored, namely, y_8 = the %-yield of 2,6-dimethoxyphenyl acetate **8**, y_9 = the %-yield of 1-(4-hydroxy-2,6-dimethoxyphenyl)-ethanone **9**, y_{10} = the %-yield of 3-hydroxy-2,6-dimethoxyphenyl acetate **10** and y = the %-decomposition, that is $y = 100 - y_{\text{not conv.}} - y_8 - y_9 - y_{10}$ and present a complete mass balance for each single experiment of Table 1.

A full factorial 2^k design **D** with $k = 3$ experimental variables (x_1, x_2 and x_3), each explored at two distinct experimental levels, denoted as $x_{k,L} = -1$ and $x_{k,H} = +1$ (the actual numerical values are provided in the footnote a of Table 1). In addition, $c = 3$ experiments were placed in the centre of the experimental

Table 2. Estimated parameter values for the models, Eqn (2) for the responses y_8, y_9, y_{10} and y

Coefficient	Model parameters[a] (model at $t = 30$ min)			
	y_8	y_9	y_{10}	y
β_0	3.2909	22.9455	4.6273	6.2727
β_1	1.4125	16.4500	5.4500	8.6250
β_2	1.0125	−0.1250	0.3250	7.1250
β_3	1.7125	−2.2750	1.1500	2.8750
β_{12}	0.8625	−0.7250	0.3250	7.1250
β_{13}	0.9625	−3.7750	1.1500	2.8750
β_{23}	0.7625	−3.7500	−0.6250	2.8750
β_{123}	0.6125	−3.8500	−0.6250	2.8750
R^2	0.977	0.940	0.902	0.912
RMSEP	0.387	3.843	1.623	3.841
RSD	0.428	4.249	1.794	4.247

[a]Responses: yield of y_8 = 2,6-dimethoxyphenyl acetate **8**, yield of y_9 = 1-(3-hydroxy-2,6-dimethoxyphenyl)ethanone **9** and yield of y_{10} = 3-hydroxy-2,6-dimethoxyphenyl acetate **10**. y = %-decomposition in total. RMSEP, root mean squared error of prediction; RSD, relative standard deviation,

domain, which ultimately provides a design matrix **D** constituted by $2^k + c = 2^3 + 3 = 11$ experiments, summarized in Table 1. The experiments were performed in a random order from which samples were withdrawn during the course of the reaction, namely, at $t = 15$, 30, 45 and 60 min. The samples were analysed by using a GC with 1,4-dinitrobenzene as an internal standard. The measured responses are tabulated adjacent to the design matrix in Table 1.

As a first stage data analysis of the determined response values, a series of line graphs showing the course of reaction (time versus yield) were produced (Fig. 1). Each of the identified compounds **8**, **9**, **10** and the decomposition are represented as separate plots, from which it is evident that the reaction time should be kept within a range of 15–30 min in order to achieve high outcomes of **8** and **9**. Prolonged reaction time results in concerted oxidation

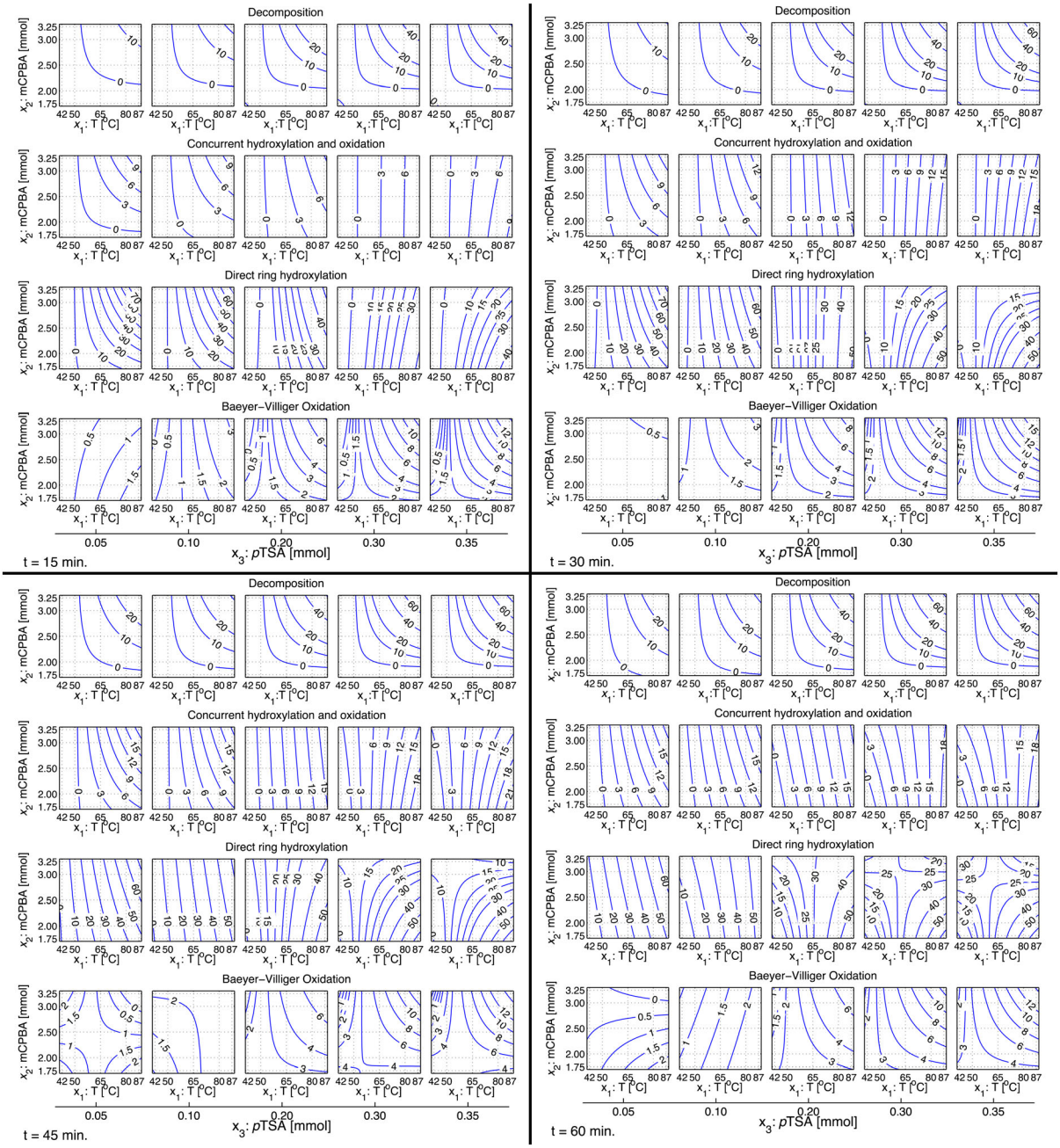

Figure 2. *Iso*-contour projections of the response surfaces (yield) for the Baeyer–Villiger oxidation [2,6-dimethoxyphenyl acetate **8**], the direct ring hydroxylation [1-(3-hydroxy-2,6-dimethoxyphenyl)ethanone **9**], concurrent hydroxylation and oxidation [3-hydroxy-2,6-dimethoxyphenyl acetate **10**], and product decomposition. The figure is composed of four subplot collections (at reaction time $t \in [15, 30, 45, 60]$ min), where each subplot collection are composed of a 4×5 matrix of 2D *iso*-contour maps. Each of the 2D plots displays the reaction temperature (x_1) as the abscissa and the quantity of the oxidant *m*CPBA (x_2) as ordinate. The location of the 2D plot in the horizontal direction (the outer frame) views the experimental variable quantity of *p*TSA (x_3) at five discrete experimental levels. Each of the rows shows thus a graphical representation of an empirical model derived with a basis in the experimental design in Table 1. Each row of 2D plots embodies the response (the *iso*-contour lines) – the %-yield of the Bayer–Villiger oxidation product (the first row from the bottom of the figure), the %-yield of the product from the direct hydroxylation, the %-yield of product of concurrent hydroxylation and Bayer–Villiger oxidation and finally the %-degradation products (that is converted substrate – the sum of the outcome of the three distinct oxidation/hydroxylation products)

of the acetyl group, direct ring hydroxylation and decomposition processes. Moreover, the ring hydroxylation appears to take place at a higher rate than the Baeyer–Villiger oxidation.

The second stage of the data analysis involved a multivariate correlation of the model matrix **M** (Eqn (1)) with the four responses y_8, y_9, y_{10} and y (Eqns (2) and (3)).

$$\mathbf{M} = [\mathbf{1}\,\mathbf{D}\,x_1x_2\ x_1x_3\ x_2x_3\ x_1x_2x_3] \tag{1}$$

$$\begin{aligned} \mathbf{y} &= \mathbf{Mb}, \quad \mathbf{y} \in [y, y_8, y_9, y_{10}] \\ \mathbf{b} &= \left(\mathbf{M}^T\mathbf{M}\right)^{-1}\mathbf{M}^T\mathbf{y} \end{aligned} \tag{2}$$

$$\begin{aligned} y_J = f(x_1, x_2, x_3) = \beta_0 + \beta_1x_1 + \beta_2x_2 + \beta_3x_3 + \beta_{12}x_1x_2 + \\ \beta_{13}x_1x_3 + \beta_{23}x_2x_3 + \beta_{123}x_1x_2x_3, \quad J = \mathbf{8}, \mathbf{9}, \mathbf{10}, \text{ decomp.} \end{aligned} \tag{3}$$

$$x_i = \frac{z_i - \left\{z_{i,L} + \frac{1}{2}\times\left(z_{i,H} - z_{i,L}\right)\right\}}{z_{i,H} - \left\{z_{i,L} + \frac{1}{2}\times\left(z_{i,H} - z_{i,L}\right)\right\}}, \qquad i = 1, \ldots, 3 \tag{4}$$

In order to facilitate the calculation of the regression coefficients (β_k) of the empirical mathematical model (Eqn (3)), the experimental variables x_1, …, x_3 were scaled according to Eqn (4), where x_i is the experimental variable $i = 1$, …, 3 provided in scaled units. z_i is the experimental variable, with variable $i = 1$, …, 3 given in the real unit. $z_{i,L}$ and $z_{i,H}$ denote the selected low and high experimental values in the real unit for each experimental variable, with variable $i = 1$, …, 3 (footnote a of Table 1). The estimated numerical values of the regression coefficients for the model describing the response surface at time $t = 30$ min are listed in Table 2.

Interpretation of the empirical models

The four empirical models Eqn (3) with the adjacent model parameters listed in Table 2 were used to produce the *iso*-contour projection maps of the response surfaces, where the contour lines express the yield-%. Figure 2 shows the *iso*-contour maps at reaction time $t = 15$, 30, 45 and 60 min, respectively.

The *iso*-contour projection maps of the response surfaces (Fig. 2) can clearly contribute answers to the major questions we stated at the outset of this investigation. The model can explain the course of the Baeyer–Villiger oxidation, predict the most beneficial conditions at a short reaction time, $t = 30$ min (which confirms the observations of the the raw data plot of Fig. 1). By using high experimental levels (+1) of all of the experimental variables x_1, …, x_3, a maximum outcome of ≈15% can be achieved of the Baeyer–Villiger oxidation product. However, at such reaction conditions, the degradation proceeds to an extent of >40%. The two other oxidative processes, the direct ring hydroxylation and the concurrent direct ring hydroxylation and Baeyer–Villiger oxidation occurs to an extent of 12–15% each. Even though at a low selectivity, the Baeyer–Villiger oxidation product can be prepared with the presented method.

An improved selectivity and outcome can be attained for the direct ring hydroxylation of the acetophenone. At short reaction time ($t = 30$ min), the direct ring hydroxylation is promoted by high level (+1) of x_1 and x_2 while keeping the experimental level of x_3 (the quantity of the acid catalyst *p*TSA) at a low to moderate level (−1 to 0). Under such conditions, the model predicts a yield of >70% and low quantities of the other oxidation products, namely, <1 and ≈10%, respectively. Moreover, the model predicts only a small degree (≈10%) of decomposition under these conditions.

Even though the model for the direct ring hydroxylation also predicts high yields at high levels of the acid catalyst *p*TSA (x_3), it is beneficial to keep the quantity of the *p*TSA at a lower level, because this suppresses the formation of the other oxidation products as well as the decomposition reaction.

In an attempt to further improve the optimized direct hydroxylation reaction described previously, we thought that a solid-supported strong acidic catalyst such as Amberlite IR120[27] could replace the dissolved acid catalyst *p*TSA. We assumed that this interchange could contribute to defeat the degradation of the acidic labile phenol. In fact, when Amberlite IR120 was utilized in the place of *p*TSA, almost no degradation took place. Moreover, the absence of strong acid in the reaction medium avoided the product decomposition during the work-up. In fact, the removal of the solvent by evaporation results in an increasing concentration of the *p*TSA, which accelerate the degradation rate of the phenolic products. Thus, this finding is a direct improvement of our previous protocol for the preparation of activated phenols via direct hydroxylation method.[9]

Figure 3 displays the results of experiments where various quantities of the acidic resin were used. The best outcome was achieved when an acidic resin loading versus substrate (acetophenone) corresponding to 200 mg: 1 mmol was utilized. Moreover, the reaction rate was also substantially improved towards the hydroxylated product, proving higher selectivity and yield. The Baeyer-Villiger oxidation product was only observed in minor quantities (<5%). The major part of the by-product

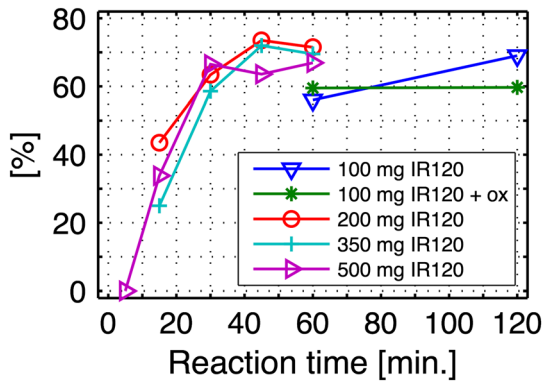

Figure 3. The effect of various loadings of the solid acid catalyst Amberlite IR120 submitting the 2,6-dimethoxy-acetophenone **7** for the *m*CPBA oxidative conditions

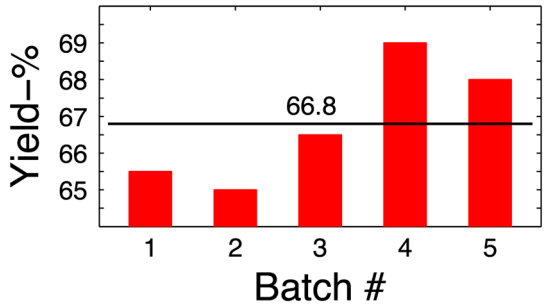

Figure 4. Investigation of the oxidation procedure by using recycled Amberlite IR120 resin. Five times use of the same resin provides a mean yield of 66.8% of the product **8**

Table 3. The substitution patterns influence on the peracid oxidation – directing direct hydroxylation mechanism or the Baeyer–Villiger oxidation mechanism

#	Substrates	#	R	Products				
					#/Yield			#/Yield
1	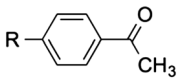	**11**	–H	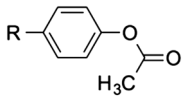	**11a**	3%	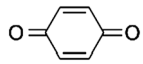	
2		**12**	$-NO_2$		**12a**	nd		
3		**13**	–CN		**13a**	nd		
4		**14**	–F		**14a**	nd		
5		**15**	$-OCH_3$		**15a**	37%		
6		**16**	$-CH_3$		**16a**	14%		
7		**17**	–OH					**17a** >99%
8	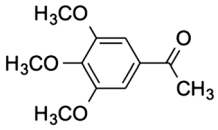	**18**	–	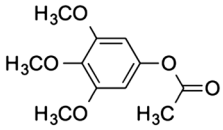	**18a**	6%	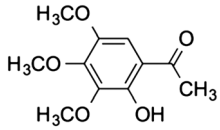	**18b** 31%
9	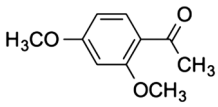	**19**	–	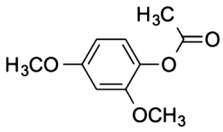	**19a**	38%	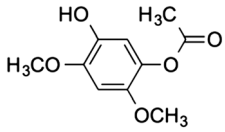	**19b** 4%
10	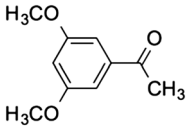	**20**	–	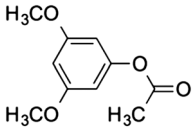	**20a**	1%	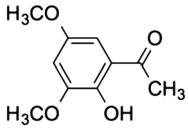	**20b** 10%
11	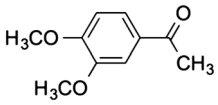	**21**	–	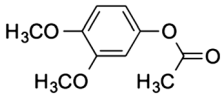	**21a**	45%	–	
12	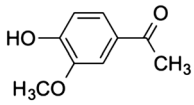	**22**	–	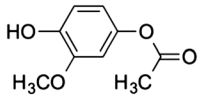	**22a**	41%	–	
13	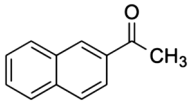	**23**	–	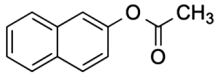	**23a**	7%	–	
14	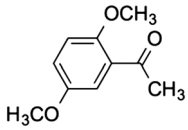	**24**	–	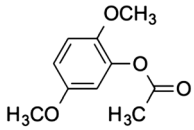	**24a**	40%	–	
15	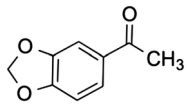	**25**	–	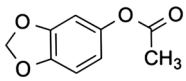	**25a**	45%	–	

meta-chloro benzoic acid, that is the reduction product from *m*CPBA, precipitate during the cooling of the post-reaction mixture, which further simplified the work-up procedure.

The acid catalyst resin was easily recycled by filtering off from the warm post-reaction mixture. The isolated resin was washed with acetonitrile and re-used without further purification, regeneration procedures or addition of more fresh resin. We repeated the reaction five times (that is four recycles of the resin). The achieved results showed only a small variance providing a yield of desired product in the range 65-69%, see Fig. 4.

The influence of the substitution pattern

The kinetics of the Baeyer–Villiger oxidation of acetophenones has previously been studied.[28] Studies have shown that electron donating groups in conjugated positions have two contradictory effects on the reaction rate. Because of the activating effect, the lower electrophilicity of the carbonyl group ought to lower the reaction rate, but the activation results in an increased basicity of the carbonyl oxygen, which once protonated increases the electrophilicity of the carbonyl carbon promoting the peracid addition. This second effect slightly prevails and speeds up the overall mechanism.[29] A question which then arises is the following: what happens when there are more substituents on the aromatic ring and how varies the selectivity relative to the various groups position? We have tried to shed some light on this issue by exploring the electronic effects of the substituents by treating series of acetophenones **11–25** of Table 3, using the optimized oxidation protocol (as developed with acetophenone **7** using Amberlite IR 120 as the acid catalyst).

The three deactivated acetophenones **12–14** were not oxidized using the conditions developed herein. Acetophenone **11** and acetonaphthone **23** provided, as expected, only small quantities of the Baeyer–Villiger product. The phenolic derivative *p*-hydroxyacetophenone **17** and **22** showed different selectivity: the first one was completely converted to the corresponding benzoquinone **17a**, whereas the second one provided only the corresponding Baeyer–Villiger derivative. We believe that in the case of the acetophenone **17,** the formation of the quinone could be ascribed to a fast oxidation by *m*CPBA of the acetic ester intermediates.[11]

The activated acetyl position of 2,4-dimethoxyacetophenone **19** directed the reaction versus a Baeyer–Villiger mechanism; however, the activating effect of the methoxy groups in positions 2 and 4 towards the carbocyclic atom in the 4-position made the reaction product reactive, and small amounts of the corresponding hydroxylated product were recovered. The concomitant electro donating effect on the same carbon atom is not present in 2,5-dimethoxy acetophenone **24** and 3,4-methylene-dioxyaceto-phenone **25**, which only provided the Baeyer–Villiger oxidation product. On the other hand, because of the strong activation of the aromatic carbon, 3,4,5-trimethoxy-acetophenone **18** and 3,5-dimethoxy-acetophenone **20** provided the corresponding phenols as the major products, which is similar to the results obtained with our model substrate 2,6-dimethoxy-acetophenone **7**. The model interpretation from the previous discussion taken together with the results achieved during the scope of the reaction investigation, it comes clear that the Baeyer–Villiger and direct ring hydroxylation mechanisms can compete depending both on the experimental conditions and on the effects of the aromatic ring substituents. It is evident that the presence of electron donating groups on the aromatic ring drives the oxidation towards the most activated carbocyclic carbon. When there is the concomitant activating effect of the two groups in the meta position to each other, the oxidation shows high selectivity on the respective activated carbocyclic carbon, achieving mostly the corresponding phenol or Baeyer–Villiger product. Nevertheless, by means of a fine-tuning of the experimental variables, we are able to maximize the yields of the corresponding phenol or Baeyer–Villiger products when the two mechanisms are in a competition.

CONCLUSIONS

We have investigated the selectivity of the peracid oxidation of substituted acetophenones. Depending on the nature of the substituents of the acetophenone, the direct aromatic ring hydroxylation can compete with the Baeyer–Villiger oxygen insertion. By means of multivariate modelling of designed experiments with 2,6-dimethoxy-acetophenone as model substrate, we could establish predictive empirical models from which it was possible to device the favoured oxidation pathway by fine-tuning the settings of the various experimental variables. Then, the protocol that provided the highest yield of the corresponding phenol was used to investigate a library of various acetophenones with the goal to explore the electronic effect of the substituents depending on their relative positions on the aromatic ring. We revealed that both the molecular structure of the substrate and the experimental conditions demonstrated a considerable impact on whether the oxidation reaction follows the oxygen insertion or the direct ring hydroxylation mechanism, particularly the synergic activation by strong electron donating group can drive the selectivity of oxygen attack. Besides revealing the various mechanistic issues, we revealed an improved protocol for the direct aromatic ring hydroxylation.

CONFLICT OF INTEREST

The authors have no conflict of interest to declare.

Acknowledgements

Economic support from the Department of Chemistry at University of Bergen and the Department of Chemistry, Materials and Chemical Engineering at Politecnico di Milano are gratefully acknowledged. H.R.B. acknowledges the Faculty of Mathematics and Natural Sciences at University of Bergen for funding to a sabbatical leave in 2013 where the project disclosed herein was completed.

REFERENCES

[1] H. Fiege1, H.-W. Voges, T. Hamamoto, S. Umemura, T. Iwata, H. Miki, Y. Fujita, H.-J. Buysch, D. Garbe, W. Paulus, Phenol Derivatives, *Ullmann's Encyclopedia of Industrial Chemistry*, Wiley, **2014**.

[2] *Phenolic Compound Biochemistry* (Eds: W. Vermerris, R. Nicholson), Springer, Dordrecht, The Netherlands, **2006**.

[3] *Encyclopedia of Agrochemicals* (Eds: J. R. Plimmer), Wiley, Hoboken, New Jersey, USA, **2002**.

[4] *Flavourings* (Eds: H. Ziegler), *Wiley-VCH*, Weinheim, Germany, **2007**.

[5] a)*The chemistry of phenols, Patai Series: The Chemistry of Functional Groups* (Eds: Z. Rappoport), Wiley, Chichester, England, **2003**. b) P. W. Kopf, Phenolic Resins, *Encyclopedia of Polymer Science and Technology*, Wiley, Weinheim, **2002**.

[6] *Handbook of Antioxidants* (Eds: E. Cadenas L. Packe), Marcel Dekker, Taylor & Francis, New York, USA, **2002**.

[7] H. Hock, S. Lang, *Ber. Dtsch. Chem. Ges.* **1944**, *B77*, 257–264.
[8] a) A. Baeyer, V. Villiger, *Ber. Dtsch. Chem. Ges.* **1899**, *32*, 3625–3633; b) A. Baeyer, V. Villiger, *Ber. Dtsch. Chem. Ges.* **1900**, *33*, 858–864; c) W. von E. Doering, E. Dorfman, *J. Am. Chem. Soc.* **1953**, *75*, 5595–5598; d) G. R. Krow, *Org. React*. **1993**, *43*, 251; e) M. Renz, B. Meunier, *Eur. J. Org. Chem.* **1999**, 737–750.
[9] H.-R. Bjørsvik, G. Occhipinti, C. Gambarotti, L. Cerasino, V. R. Jensen, *J. Org. Chem.* **2005**, *70*, 7290–7296.
[10] a) T. W. Lyons, M. S. Sanford, *Chem. Rev.* **2010**, *110*, 1147–1169; b) W. Wu, H. Jiang, *Acc. Chem. Res.* **2012**, *45*, 1736–1748; c) G. Shan, X. Yang, L. Ma, Y. Rao, *Angew. Chem.* **2012**, *124*, 13247–13251.
[11] R. Rodríguez Gonzáles, C. Gambarotti, L. Liguori, H.-R. Bjørsvik, *J. Org. Chem.* **2006**, *71*, 1703–1706.
[12] G. Occhipinti, L. Liguori , A. Tsoukala, H.-R. Bjørsvik, *Org. Process Res. Dev.* **2010**, *14*, 1379–1384.
[13] A. Tsoukala, H.-R. Bjørsvik, *Org. Process Res. Dev.* **2011**, *15*, 673–680.
[14] P. Metivier, *Friedel-Crafts Acylation in Friedel–Crafts Reaction*. (Eds: R. A. Sheldon, H. Bekkum, Wiley-VCH, New York, **2001**, 161–172.
[15] See for example: E. K. Euranto, *Esterification and Ester Hydrolysis, In Carboxylic Acids and Esters* (Ed: S. Patai), Wiley, Chichester, UK, **1969**.
[16] a) K. Fries, G. Finck, *Chem. Ber.* **1908**, *41*, 4271–4284; b) K. Fries, W. Pfaffendorf, *Chem. Ber.* **1910**, *43*, 212–219; c) A. Commarieu, W. Hoelderich, J. A. Laffitte, M.-P. Dupont, *J. Mol. Cat. A.: Chemical*. **2002**, *182–183*, 137–141; d) S. Paul, M. Gupta, *Synthesis*. **2004**, 1789–1792; e) I. Jeon, I. K. Mangion, *Synlett*. **2012**, *23*, 1927–1930.
[17] a) H.-J. Knölker, *W. Fröhner. Tetrahedron Lett.* **1997**, *38*, 4051–4054; b) H.-J. Knölker, W. Fröhner, *J. Chem. Soc. Perkin Trans. 1*. **1998**, 173–175.
[18] a) H.-J. Knölker, K. R. Reddy, A. Wagner, *Tetrahedron Lett.* **1998**, *39*, 8267–8270; b) H.-J. Knölker, W. Fröhner, K. R. Reddy, *Synthesis* **2002**, 557–564.
[19] F. Mo, L. J. Trzepkowski, G. Dong, *Angew. Chem. Int. Ed.* **2012**, *51*, 13075–13079.
[20] R. Zaninetti, S. V. Cortese, S. Aprile, A. Massarotti, P. L. Canonico, G. Sorba, G. Grosa, A. A. Genazzani, T. Pirali, *ChemMedChem*. **2013**, *8*, 633–643.
[21] R. Criegee, *Justus Liebigs Ann. Chem.* **1948**, *560*, 127–135.
[22] H.-J. Knölker, W. Fröhner, K. R. Reddy, *Eur. J. Org. Chem*. **2003**, 740–746.
[23] a) G. E. P. Box, W. G. Hunter, J. S. Hunter, *Statistics for Experimenters. An Introduction to Design, Data Analysis, and Model Building*, Wiley, New York, **1978**;
b) G. E. P. Box, N. R. Draper, *Empirical model-building and response surfaces*Wiley, New York, **1987**.
[24] a) N. R. Draper, H. Smith, *Applied Regression Analysis*3rd edn. Wiley, New York, **1998**; b)D. C. Montgomery, E. A. Peck, *Introduction to Linear Regression Analysis*, Wiley, New York, **1982**.
[25] See for example: a)*Base SAS® 9.2 Procedures Guide*. SAS Institute Inc, Cary, NC, **2009**. b) *SAS/GRAPH® 9.2: Statistical Graphics Procedures Guide*2nd edn. SAS Institute Inc, Cary, NC, **2010**.
[26] See for example: a)*Using MATLAB, Version 6*, Natick, MA, The MathWorks, Inc, **2000**. b)*Using MATLAB Graphics, Version 6*, Natick, MA, The Matwork, Inc., **2000**. c) D. Hanselman, B. Littlefield, *Mastering MATLAB: A Comprehensive Tutorial and Reference*Prentice-Hall Inc, Upper Saddle River, NJ, **1996**.
[27] Amberlite IR120 is a gel type, strongly acidic, cation exchange resin of the sulfonated polystyrene type. The resin we used held 4.7 mmol sulphonic acid groups per gram of the resin.
[28] a) J. Meinwald, H. Tsuruta, *J. Am. Chem. Soc.* **1970**, *92*, 2580–2581; b) Y. Ogata, Y. Sawaki, *J. Org. Chem.* **1972**, *37*, 2953–2957.
[29] L. Reyes, J. R. Alvarez-Idaboy, N. Mora-Diez, *J. Phys. Org. Chem.* **2009**, *22*, 643–649.

SUPPORTING INFORMATION

Additional supporting information may be found in the online version of this article at the publisher's website.

Supporting Information

The Baeyer-Villiger oxidation versus aromatic ring hydroxylation: Competing organic peracid oxidation mechanisms explored by multivariate modelling of designed multi-response experiments

Cristian Gambarotti[a] and Hans-René Bjørsvik[b,*]

[a]*Department of Chemistry, Materials, and Chemical Engineering, Politecnico di Milano, Piazza Leonardo da Vinci 32, I-20133 Milan, Italy*
[b]*Department of Chemistry, University of Bergen, Allégaten 41, N-5007 Bergen, Norway*

*e-mail: hans.bjorsvik@kj.uib.no, phone +47 55 58 34 52, fax +47 55 58 94 90

[*] To whom correspondence should be sent

^{1}H-NMR of 1-(3-hydroxy-2,6-dimethoxyphenyl)ethan-1-one (9)

^{1}H NMR (400 MHz, $CDCl_3$): δ 2.52 (s, 3 H, CH_3), 3.77 (s, 3 H, CH_3), 3.81 (s, 3 H, CH_3), 5.32 (s, 1 H, OH), 6.59 (d, J = 8.8 Hz, 1 H, CH), 6.92 (d, J = 8.8 Hz, 1 H, CH) ppm.

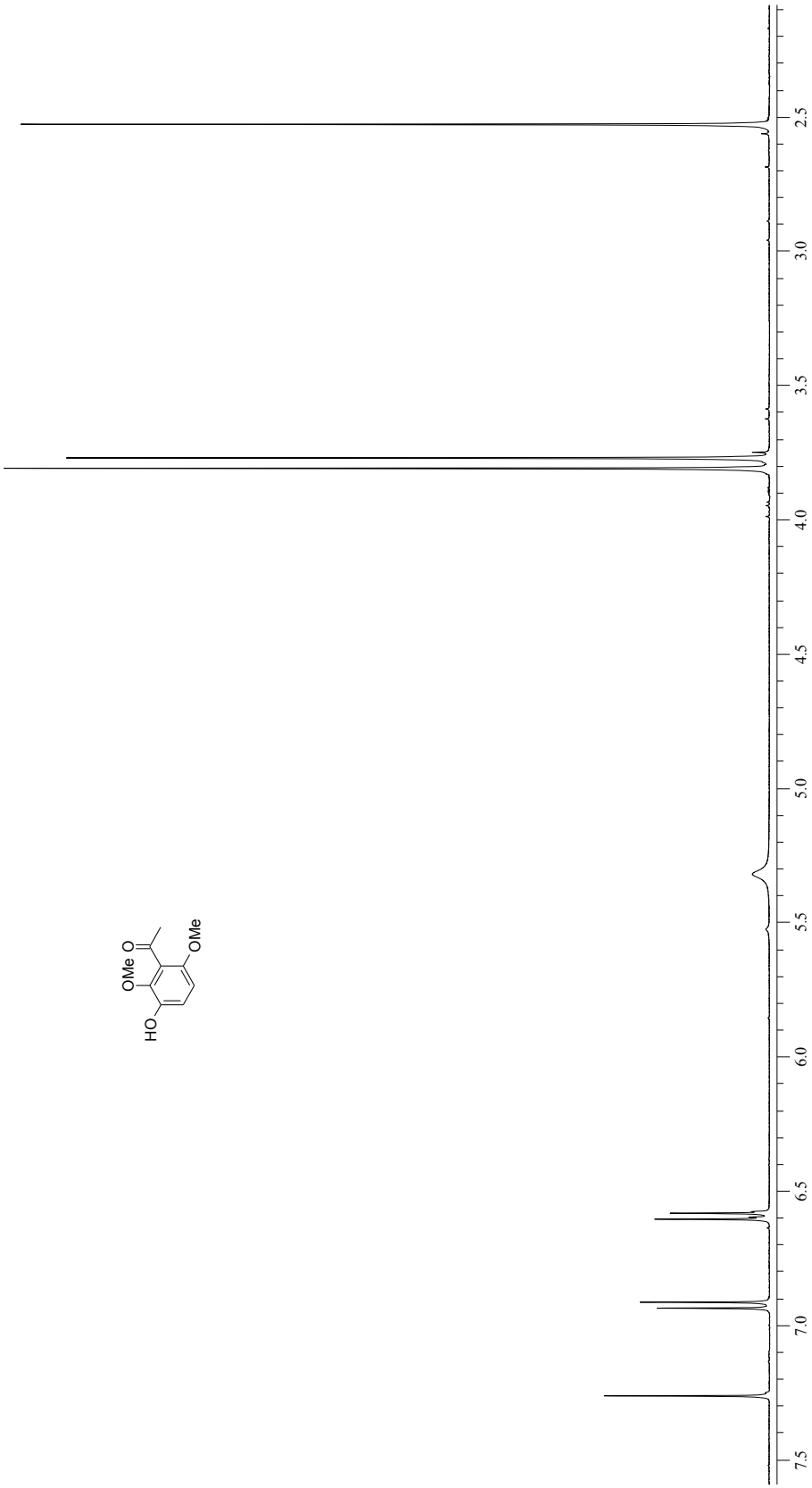

^{13}C-NMR of 1-(3-hydroxy-2,6-dimethoxyphenyl)ethan-1-one (9)

^{13}C NMR (100 MHz, $CDCl_3$): δ 32.3, 56.3, 62.9, 107.7, 116.3, 125.5, 143.0, 143.8, 150.0, 201.8 ppm.

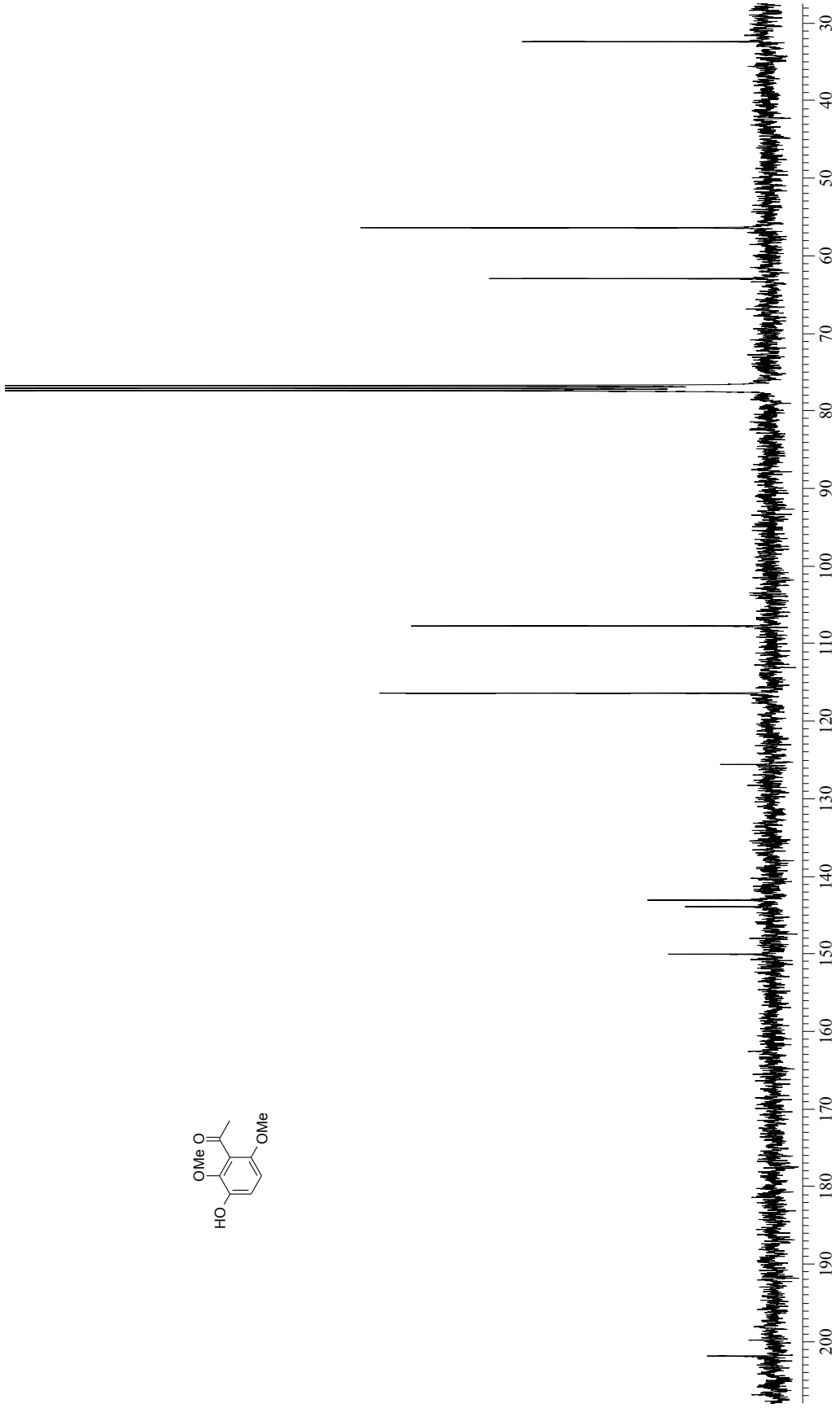

MS of 1-(3-hydroxy-2,6-dimethoxyphenyl)ethan-1-one (9)

Mass spectra recorded by a GC-MS analysis using an Agilent 6890 Gas Chromatograph (GC) system equipped with a 30 m × 0.250mm HP-5MS GC column and an Agilent 5973 Mass Selective Detector (MSD).

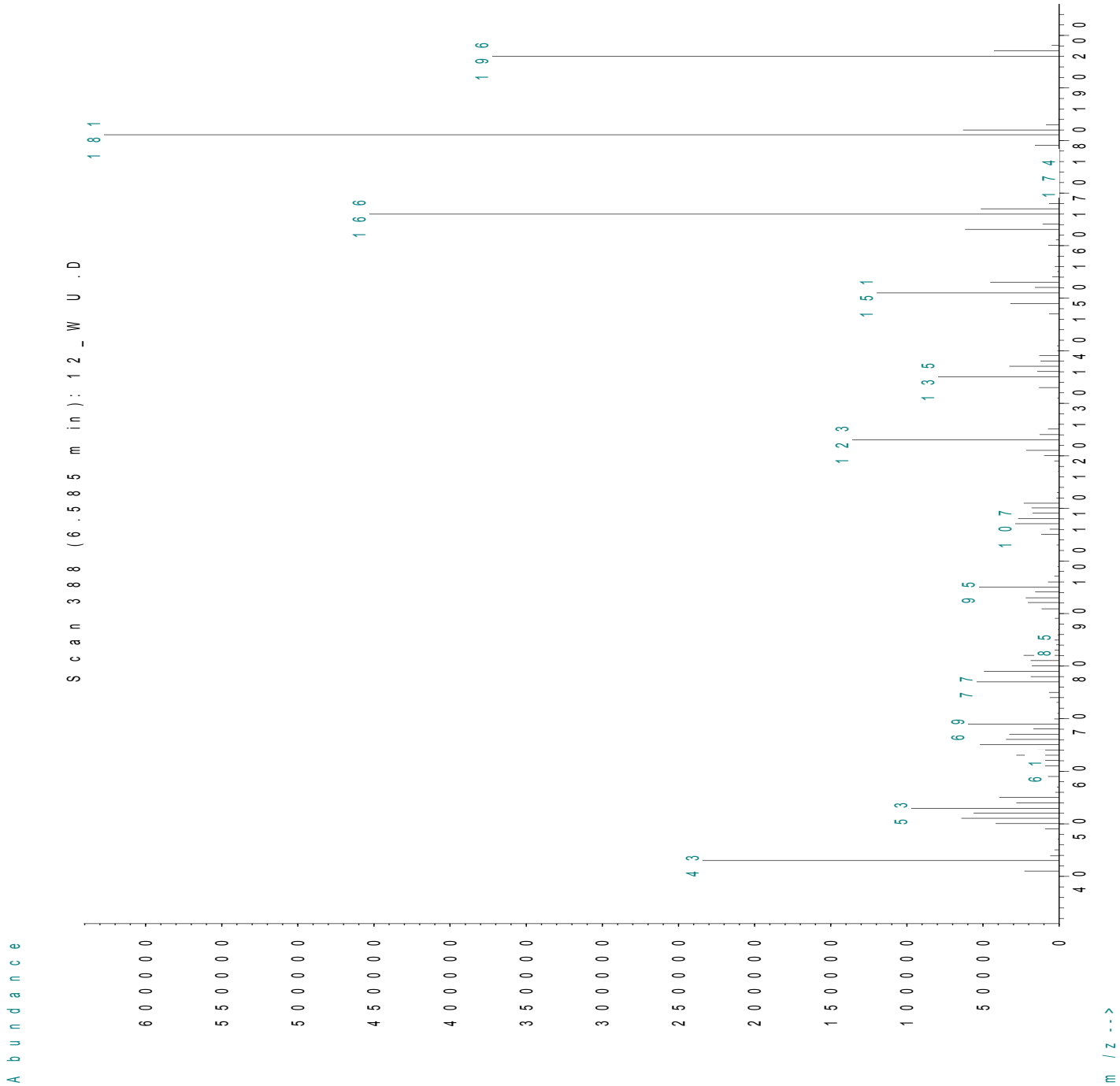

MS of 2,6-dimethoxyphenyl acetate (8)

CAS 944-99-0, ref. MS spectra available on Scifinder

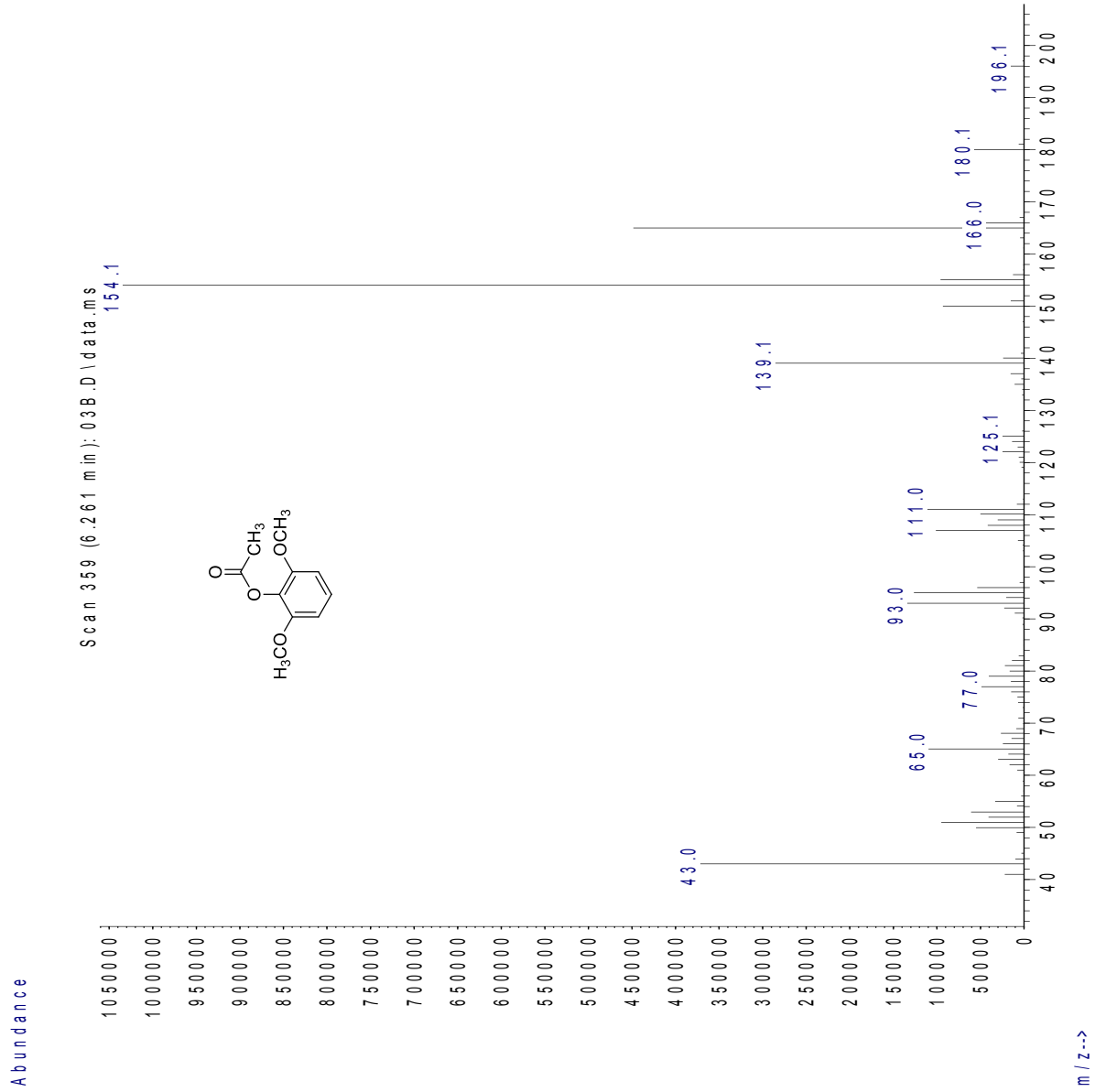

MS of 1-(3-hydroxy-2,6-dimethoxyphenyl)ethanone (9)

CAS 56358-74-8, *J. Org. Chem*. **2005**, *70*, 7290-7296

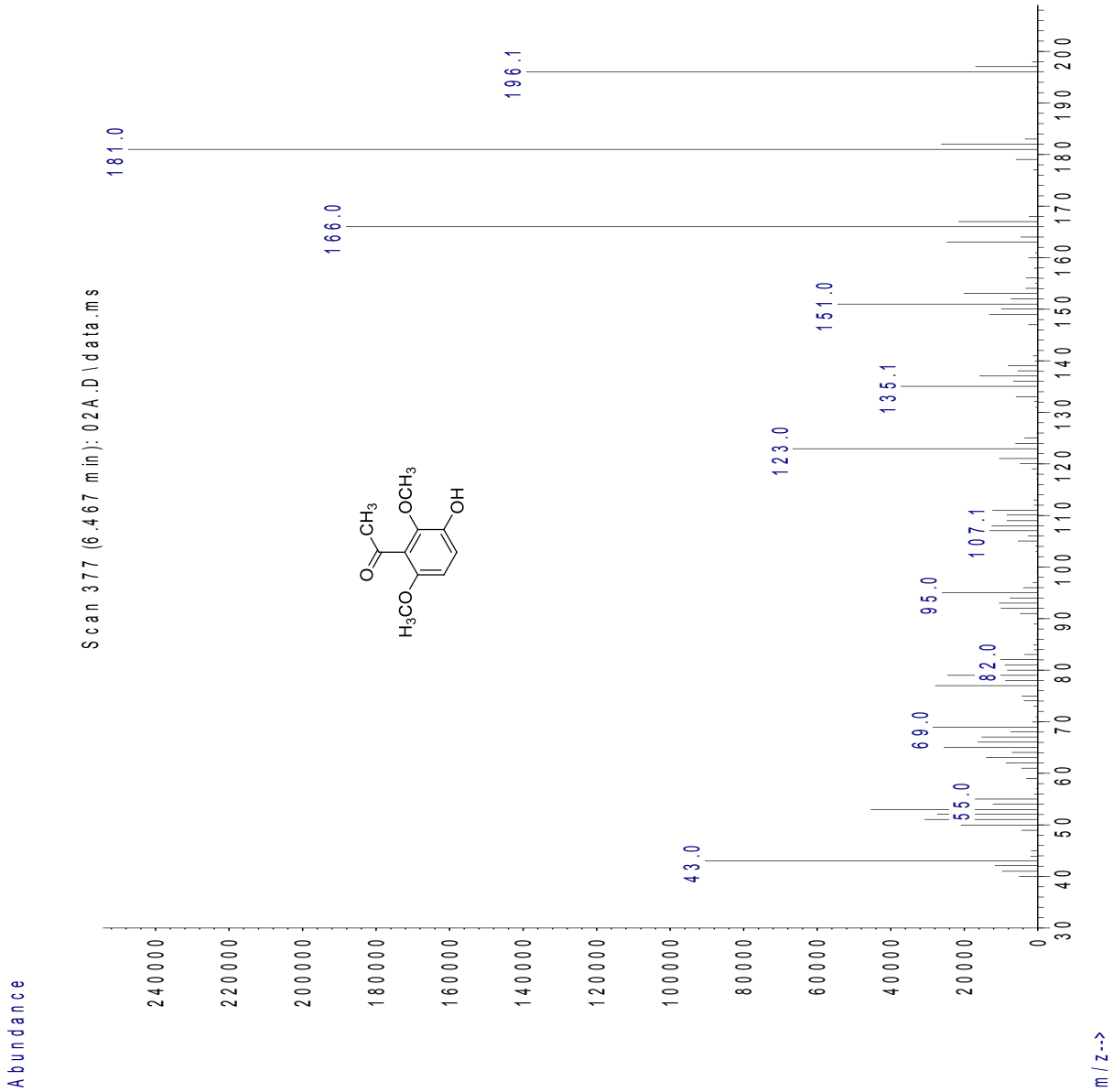

MS of 3-hydroxy-2,6-dimethoxyphenyl acetate (10)

CAS 865440-85-3, *J. Org. Chem.* **2005**, *70*, 7290-7296

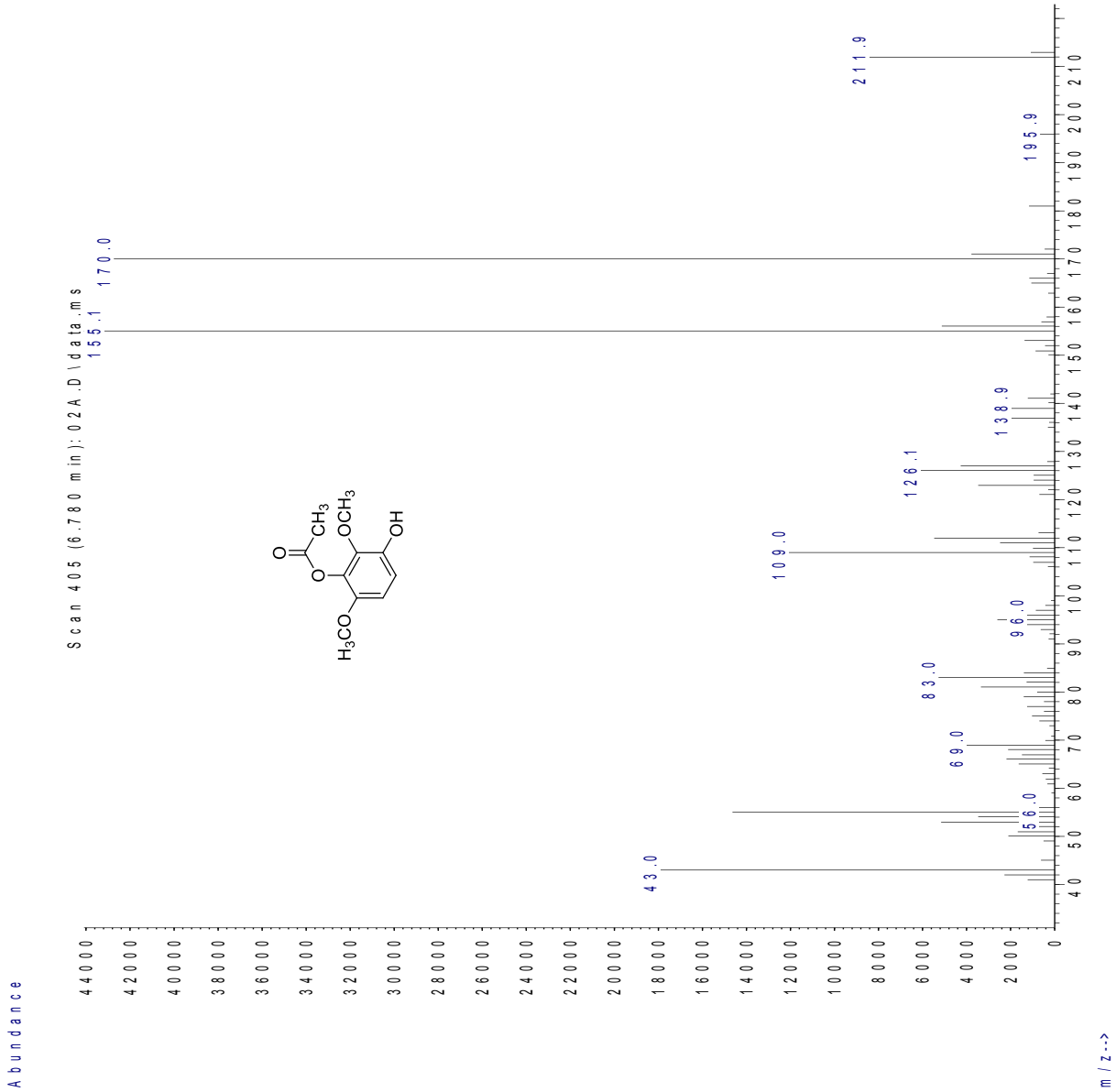

MS of Phenyl acetate (11a)

CAS 122-79-2, ref. MS spectra available on Scifinder

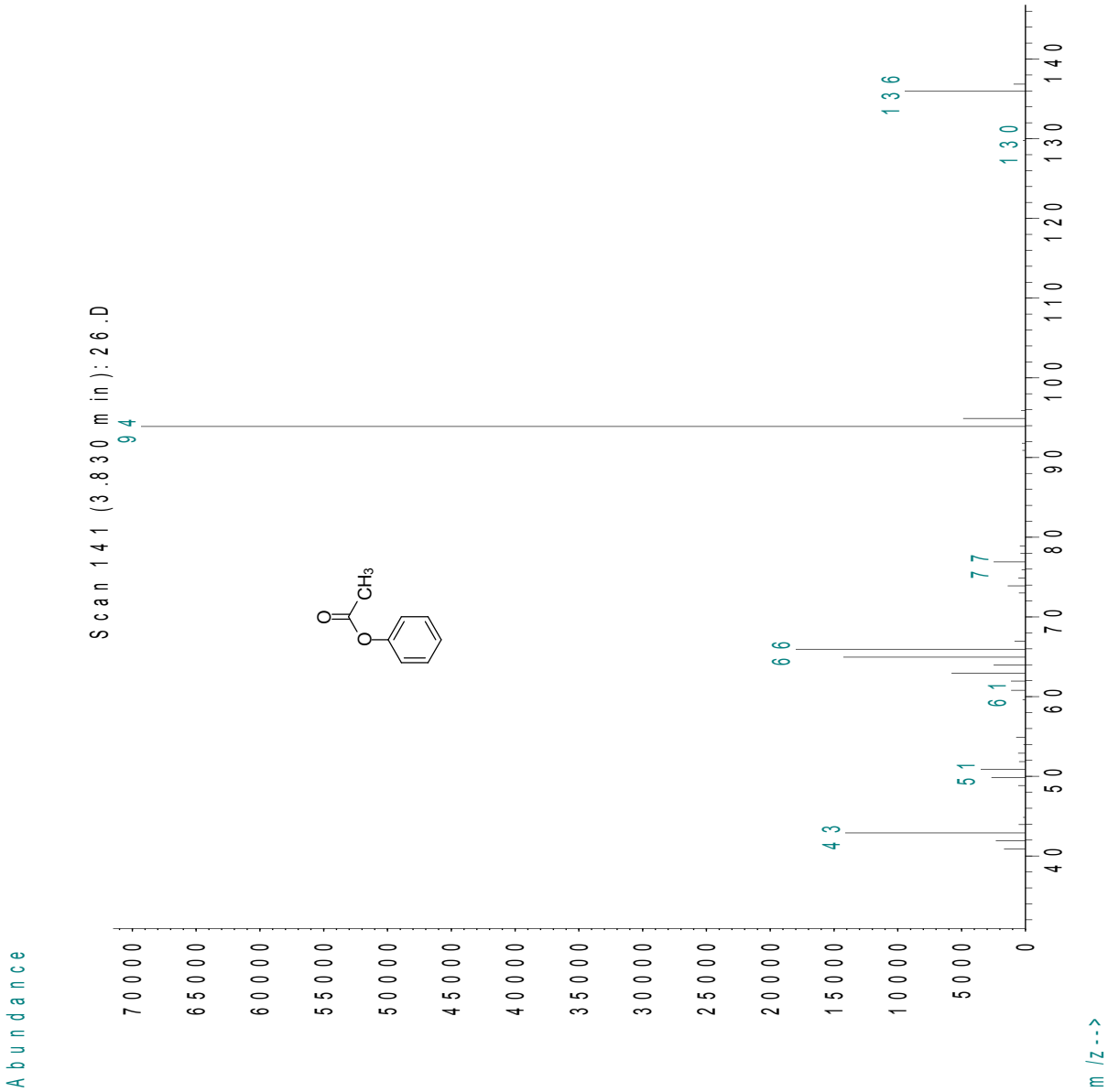

MS of 4-methoxyphenyl acetate (15a)

CAS 1200-06-2, ref. MS spectra available on Scifinder

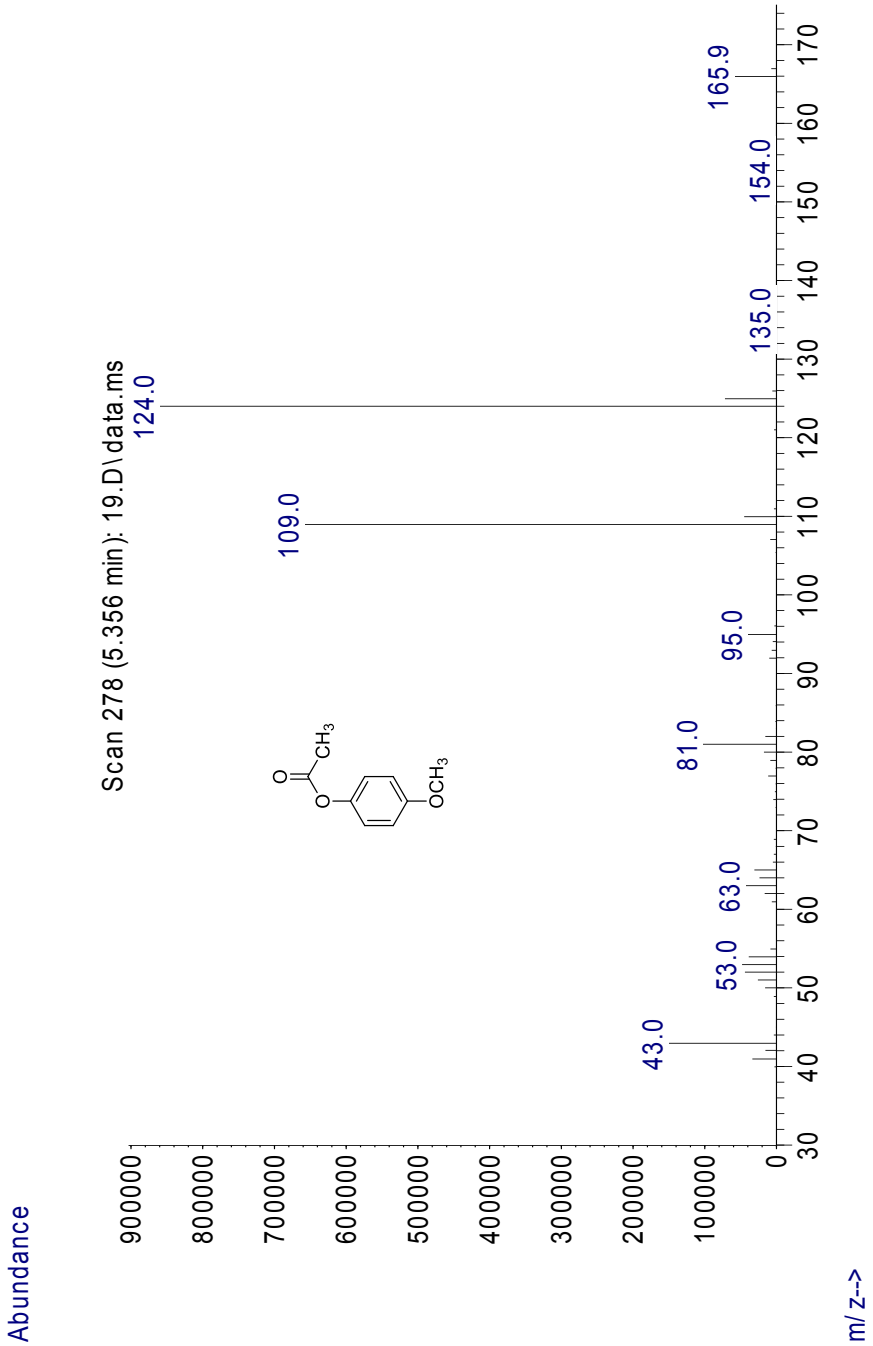

MS of *p*-Tolyl acetate (16a)

CAS 140-39-6, ref. MS spectra available on Scifinder

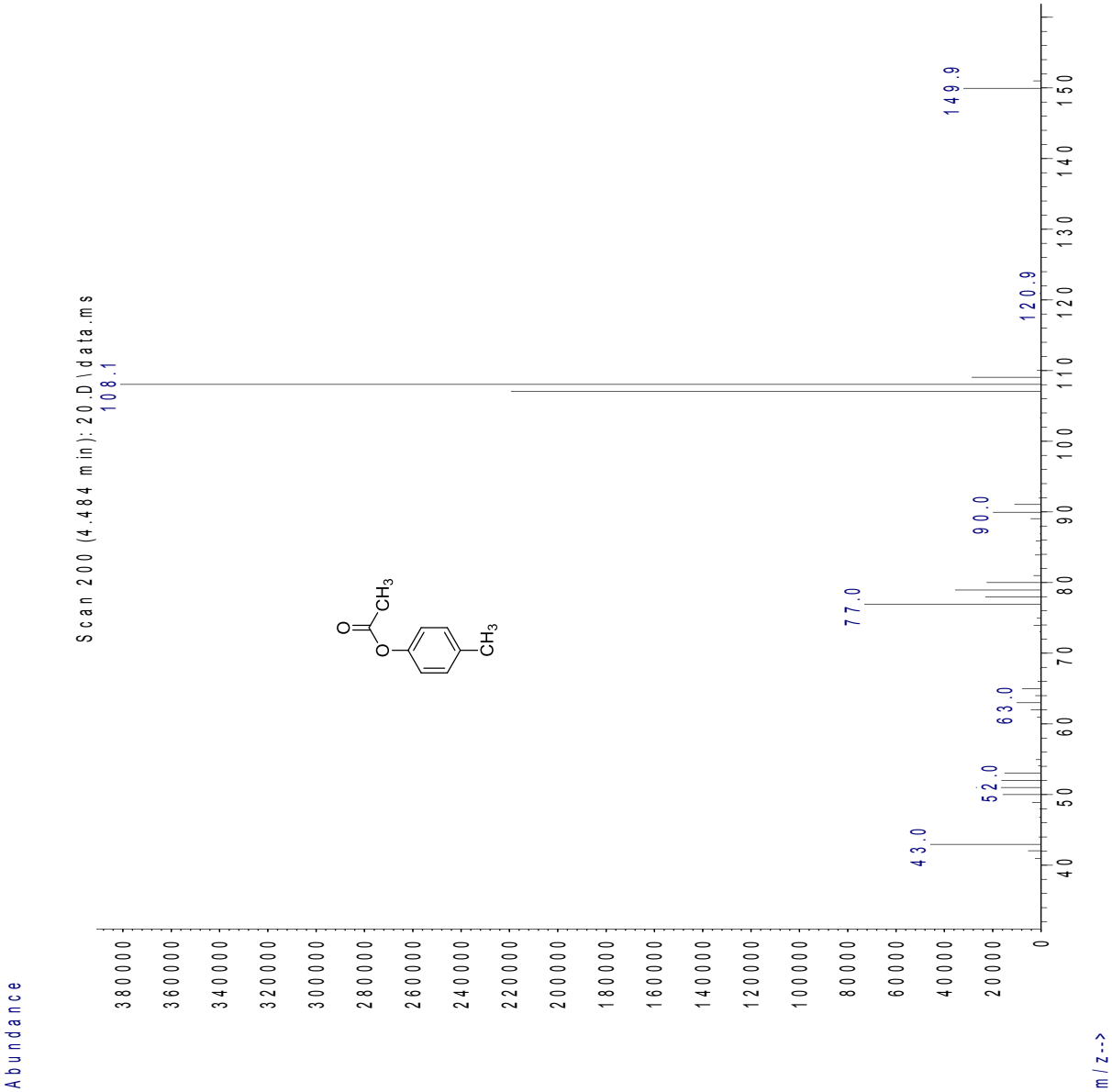

MS of Benzoquinone (17a)

CAS 106-51-4, ref. MS spectra available on Scifinder

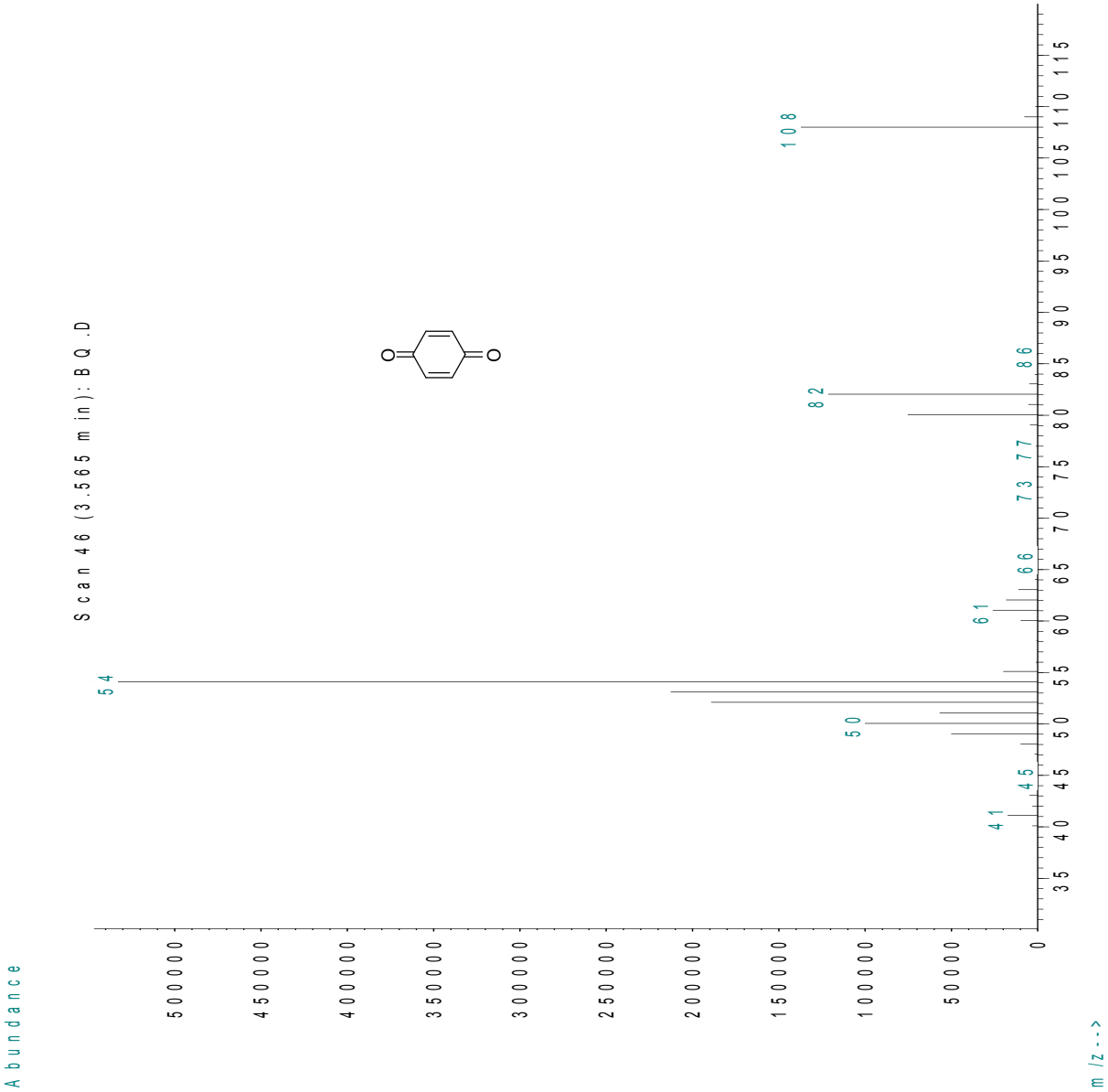

MS of 3,4,5-Trimethoxyphenyl acetate (18a)

CAS 17742-46-0, ref. MS spectra available on Scifinder

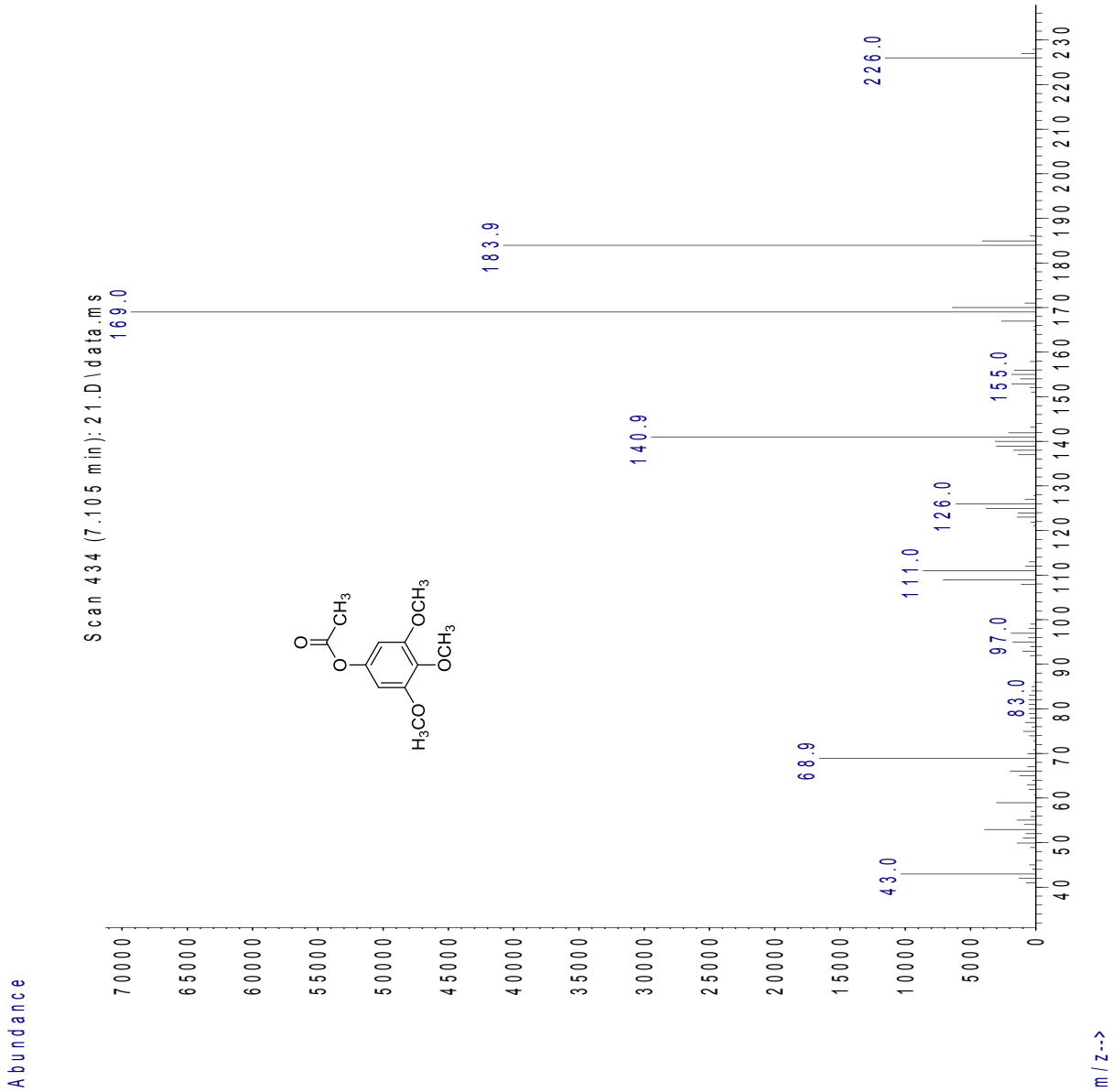

MS of 1-(2-Hydroxy-3,4,5-trimethoxyphenyl)ethanone (18b)

CAS 30225-96-8, *J. Org. Chem*. **2005**, *70*, 7290-7296

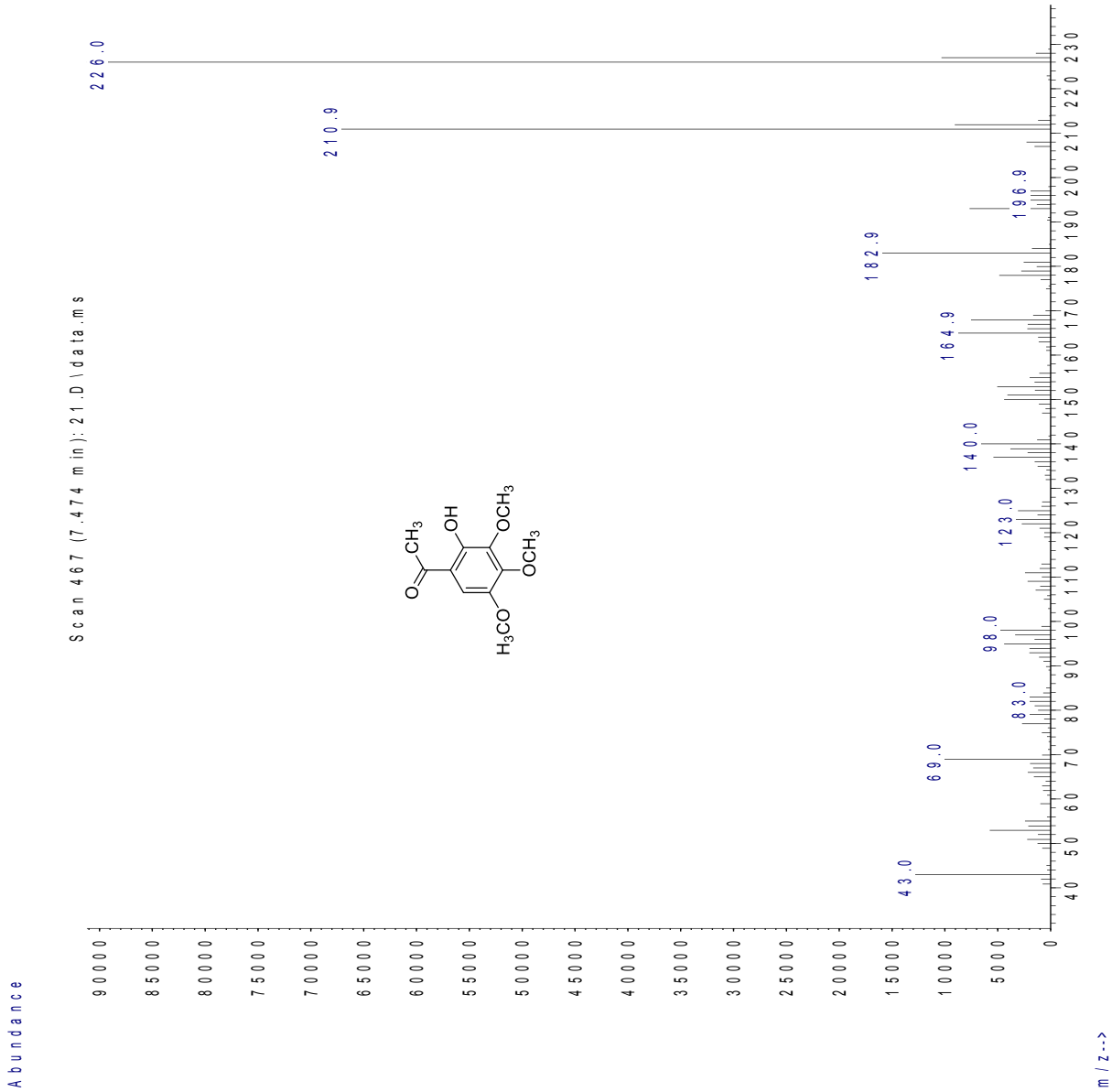

MS of 2,4-Dimethoxyphenyl acetate (19a)

CAS 27257-07-4, ref. MS spectra available on Scifinder

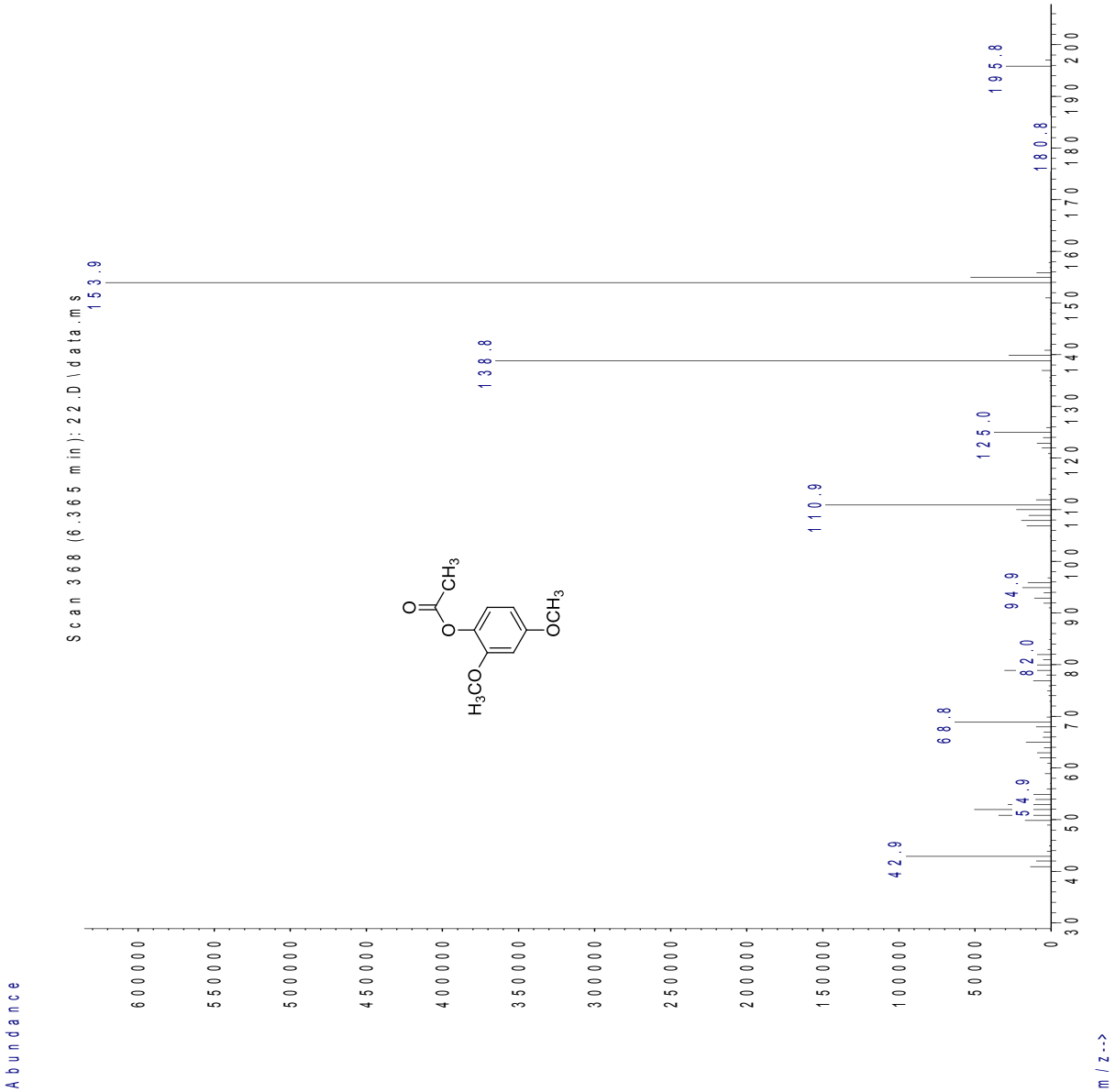

MS of 5-Hydroxy-2,4-dimethoxyphenyl acetate (19b)

evaluated by GC-MS analysis, not isolated

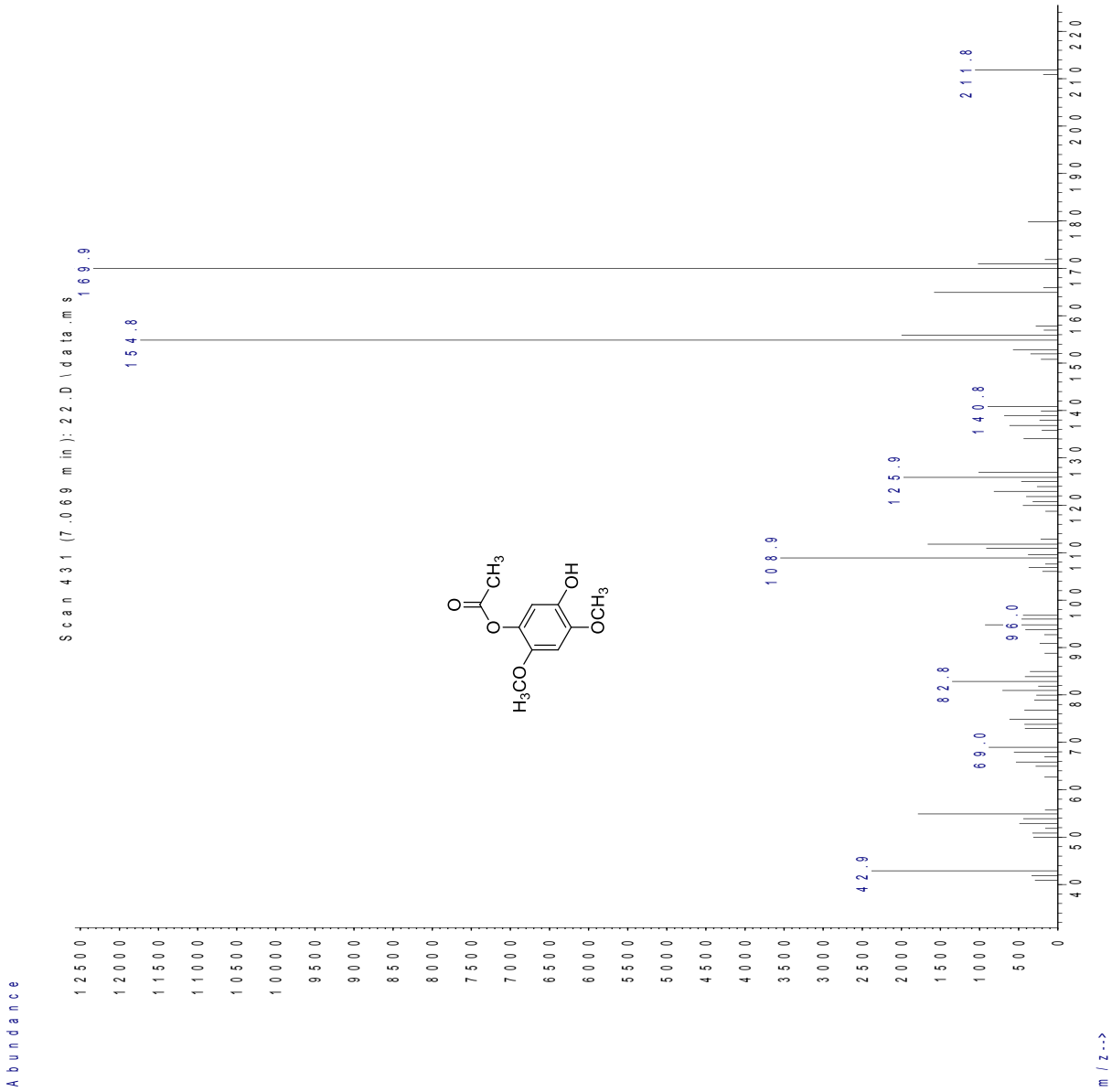

MS of 1-(2-Hydroxy-3,5-dimethoxyphenyl)ethanone (20b)

CAS 17605-00-4, *J. Org. Chem*. **2005**, *70*, 7290-7296

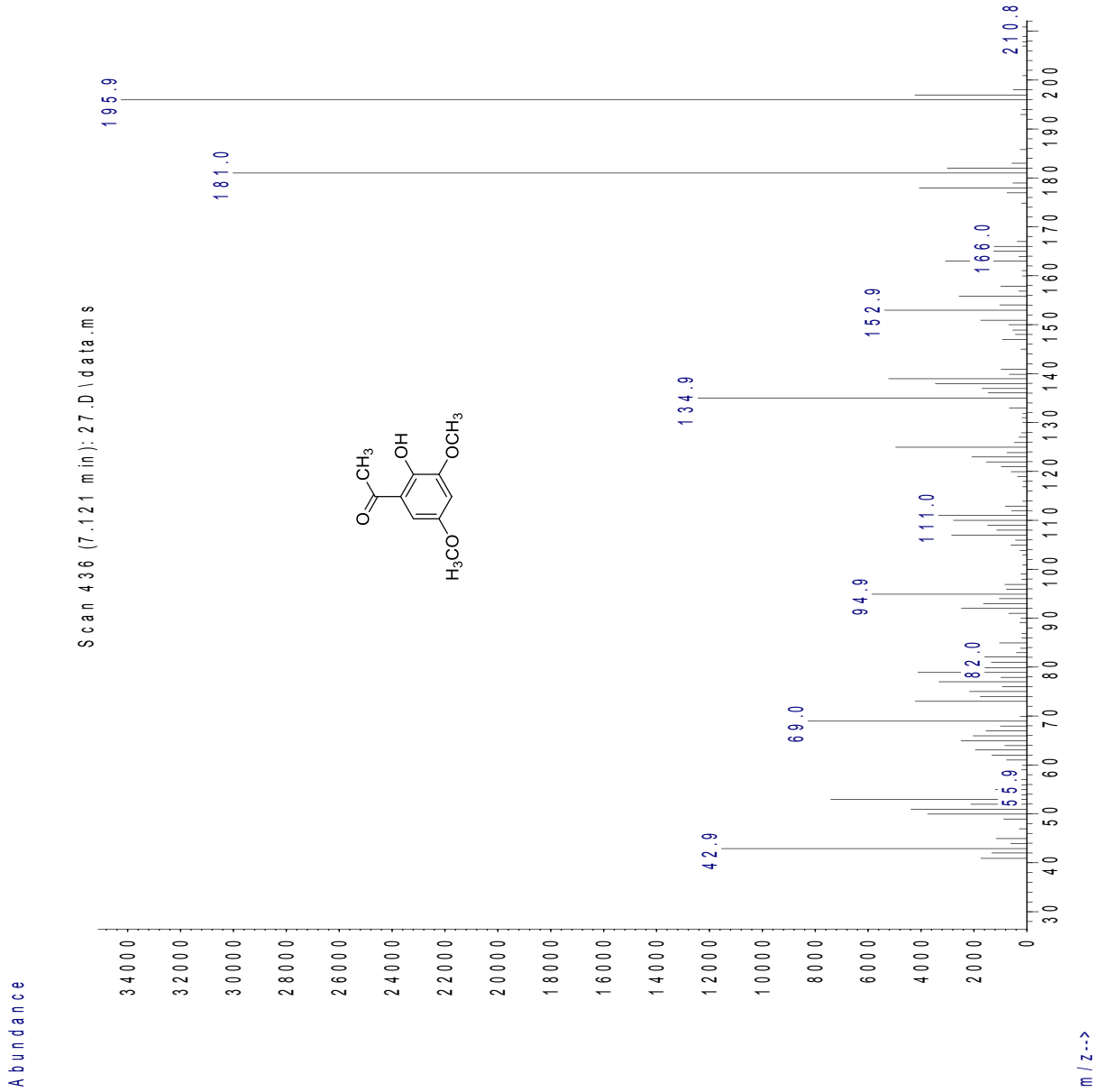

MS of 3,4-Dimethoxyphenyl acetate (21a)

CAS 7203-46-5, ref. MS spectra available on Scifinder

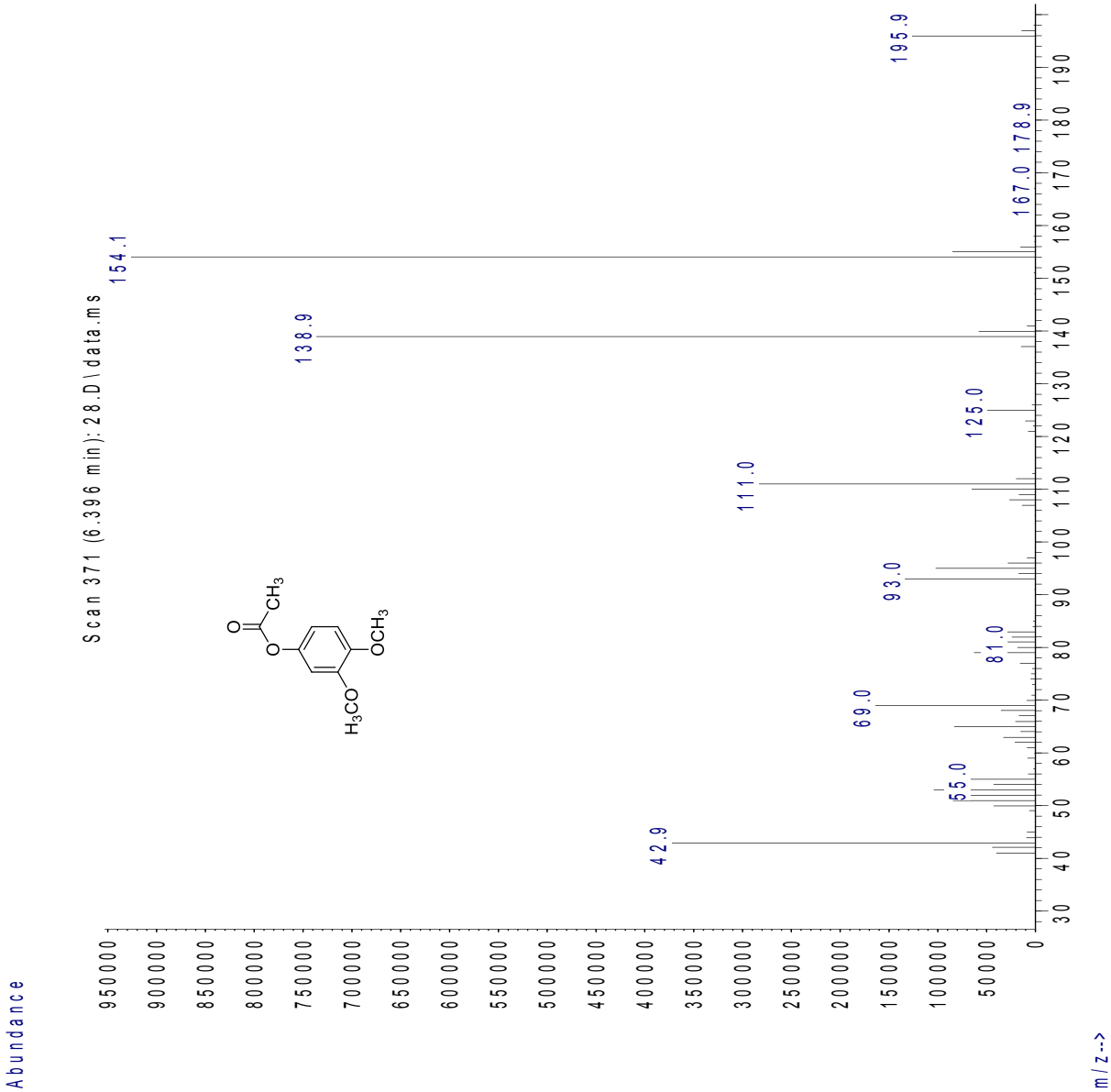

MS of 4-Hydroxy-3-methoxyphenyl acetate (22a)

CAS 57244-88-9, *The Baeyer–Villiger Oxidation of Ketones and Aldehydes*, Grant R. Krow,
DOI: 10.1002/0471264180.or043.03,

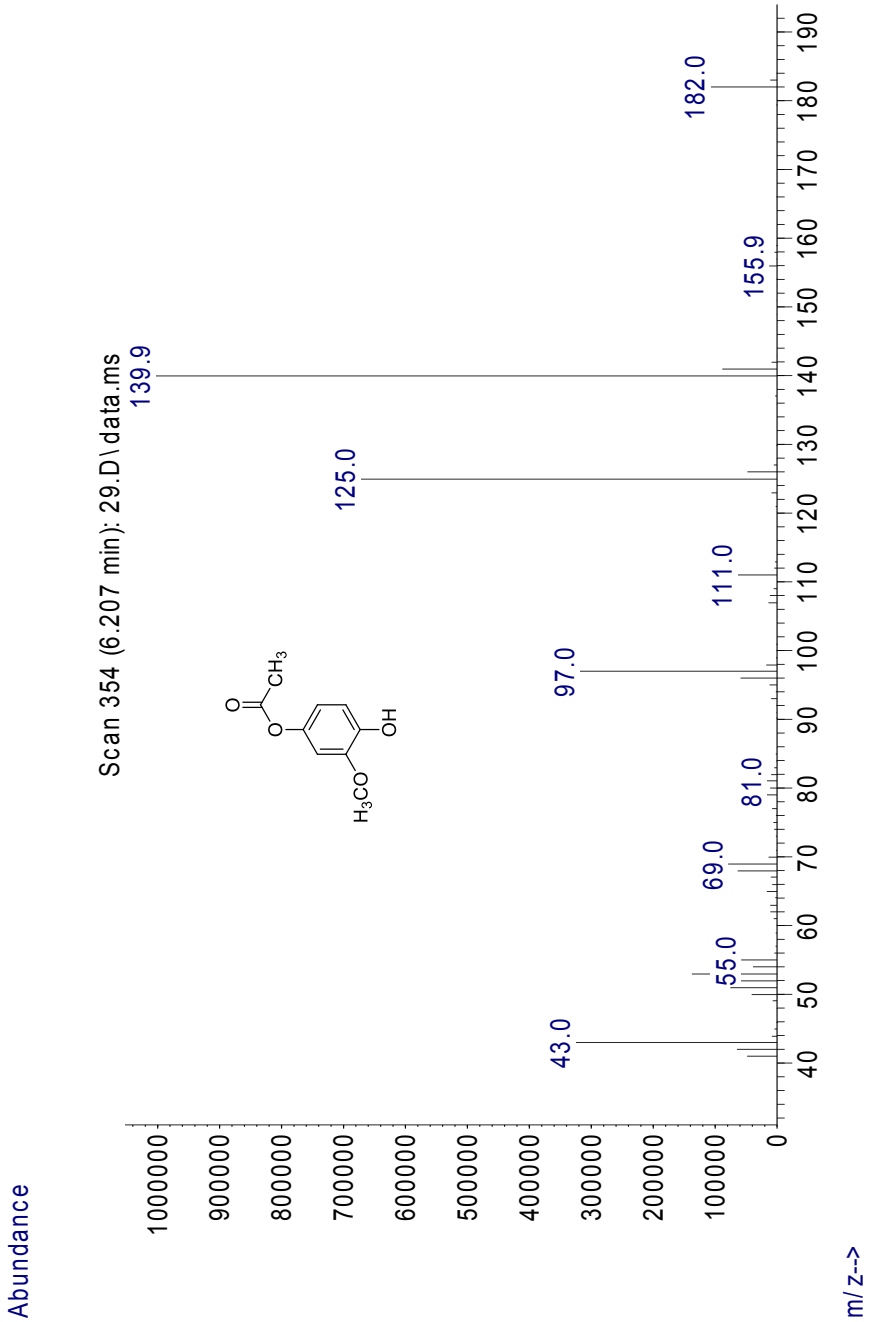

MS of Naphthalen-2-yl acetate (23a)

CAS 1523-11-1, ref. MS spectra available on Scifinder

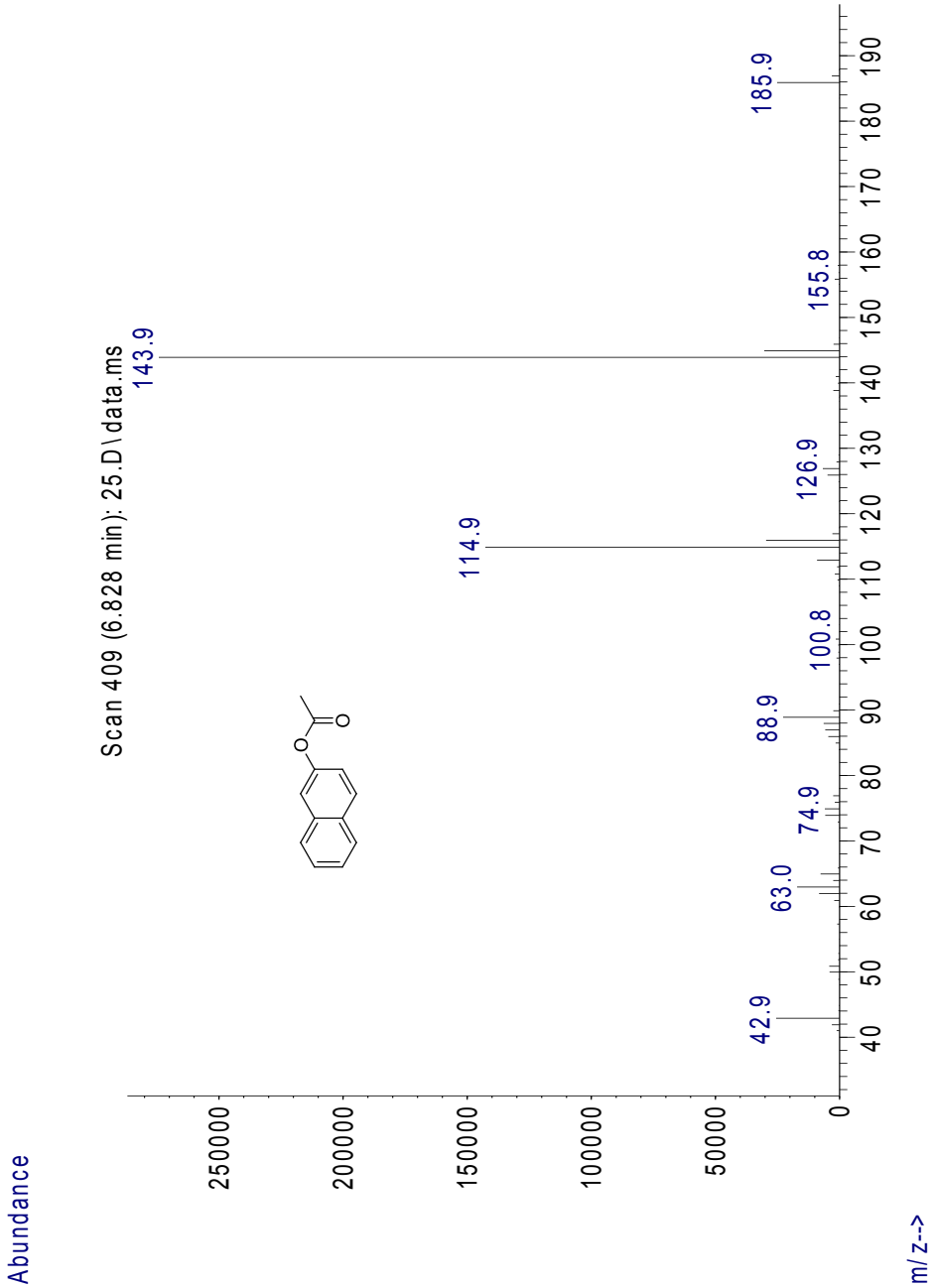

MS of 2,5-Dimethoxyphenyl acetate (24a)

CAS 27257-06-3, ref. MS spectra available on Scifinder

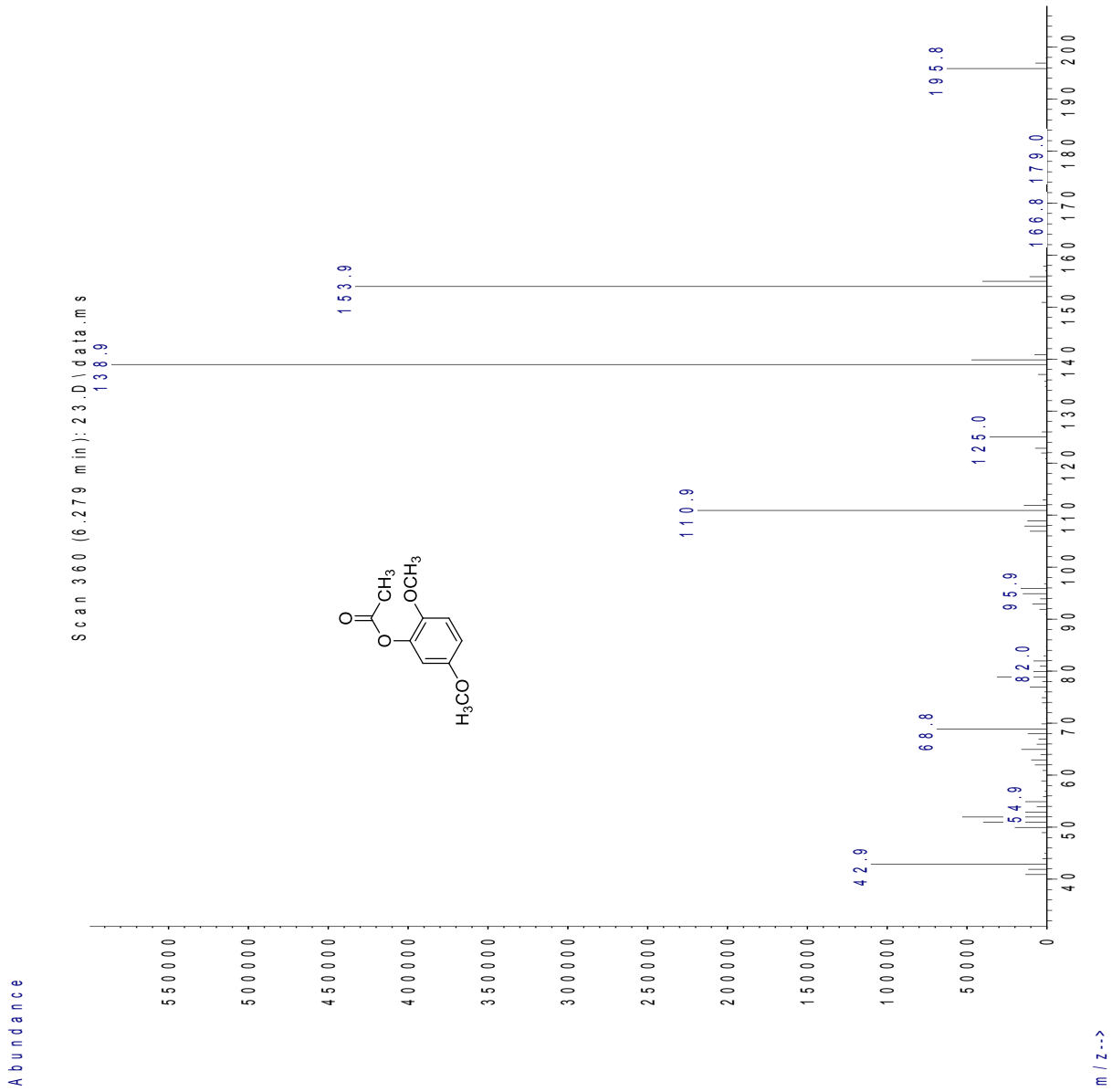

MS of Benzo[d][1,3]dioxol-5-yl acetate (25a)

(partially overlaped on 3-chlorobenzoic acid spectra),
CAS 326-58-9, *Helv. Chim. Acta* **2011**, *94*, 185-198

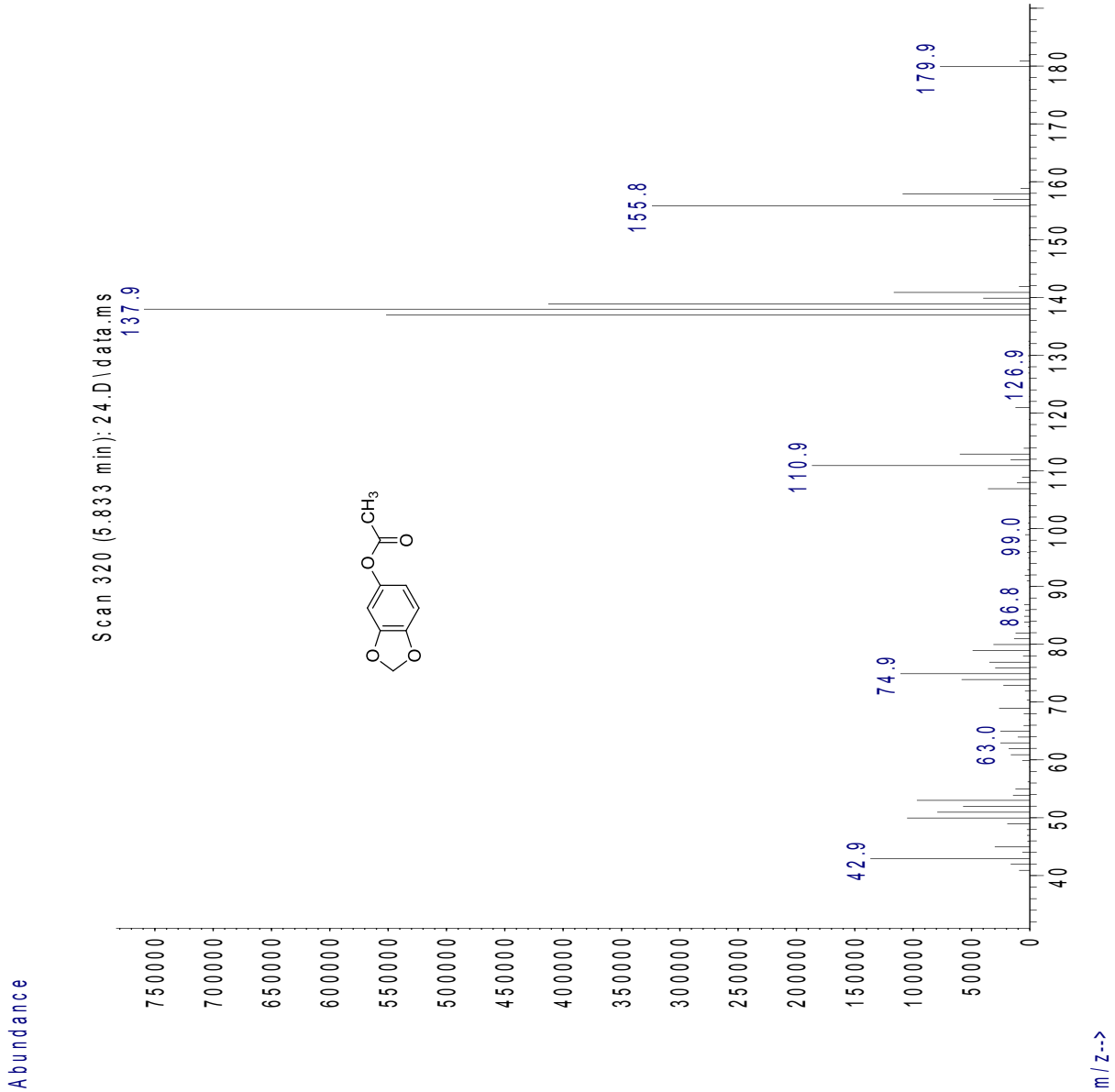

MS of 3-Chlorobenzoic acid

CAS 535-80-8